

Initial assessment of the geology and economic potential of the Tikiusaaq carbonatite complex and ultramafic lamprophyre dykes

Mineral resource assessment of the
Archaean Craton (66° to 63°30'N)
SW Greenland Contribution no. 3

Agnete Steenfelt, Frands Schjøth,
Karina K. Sand, Karsten Secher,
Sebastian Tappe, Else Moberg
& Tapani Tukiainen

(1 DVD included)



Initial assessment of the geology and economic potential of the Tikiusaaq carbonatite complex and ultramafic lamprophyre dykes

Mineral resource assessment of the
Archaean Craton (66° to 63°30'N)
SW Greenland Contribution no. 3

Agnete Steenfelt, Frands Schjøth,
Karina K. Sand, Karsten Secher,
Sebastian Tappe, Else Moberg
& Tapani Tukiainen

(1 DVD included)

Frontispiece



Partly exposed subvertical sheet of carbonatite with three metres long lens of magnetite below person. Fenitised country rock amphibolite to the right. Tikiusaaq, upper Base creek.

Contents

Frontispiece	2
Abstract	5
Introduction	6
Background.....	6
Site description and geological setting.....	8
Overview of investigations	11
Field observations.....	11
Measurement of gamma-radiation.....	11
Sampling.....	12
Processing of remotely sensed data.....	12
Chemistry and mineralogy.....	13
Isotope chemistry and age dating.....	13
Studies of kimberlite indicator minerals.....	13
Documentation of data on DVD	14
Stored information.....	14
Description of ArcMap groups and layers.....	15
Streams.....	15
Lakes.....	15
Ice.....	15
Geographical net and area frame.....	15
Field observations.....	15
Gamma-spectrometry.....	17
Data acquisition.....	17
Data presentation.....	18
Geology.....	19
Field observations.....	20
Results of gamma-spectrometry.....	22
Interpretation of remote sensing data.....	22
Interpretation of all acquired data.....	23
Mineralogy.....	23
Geochemistry.....	23
Data acquisition.....	23
Data presentation.....	25
Terrain model.....	25
Remote sensing.....	25
Aeromagnetic image.....	25
Satellite image.....	26

Results	28
Gamma-spectrometry	28
Lithological and gamma-spectrometric profiling	28
Gamma-spectrometric mapping	28
Structure and components of the Tikiusaaq complex.....	29
Carbonatite.....	31
Fenite	32
Ultramafic lamprophyre	33
Age determination	37
Mineralisation.....	38
Economic potential	43
Carbonatite	43
Ultramafic lamprophyre	43
Conclusion and recommendation	44
References	45
Appendix	46

Abstract

The Late Jurassic Tikiusaaq carbonatite complex, discovered in 2005 by GEUS, has been studied during 2006 and 2007 in the frame of a joint project between Geological Survey of Denmark and Greenland (GEUS) and the Bureau of Minerals and Petroleum (BMP), government of Greenland. The objective was to obtain information on the size, structure, composition and economic potential of the intrusive complex. All information and data acquired during field work and sample processing are documented in ESRI ArcMap format on the DVD accompanying this report. The present report describes activities undertaken and data acquired, and discusses the results.

The Tikiusaaq complex comprises massive carbonatite sheets, carbonatite veins and ultramafic lamprophyre dykes. Fracturing, alteration, carbonatite veining and impregnation cover an area of 14 by 14 km, while the area with exposure of massive carbonatite sheets is 2 by 3 km in size. Field observations together with remote sensing data suggest that parts of the massive carbonatite is hidden below glacial terraces, and more carbonatite may even exist at depth beneath the northern and eastern part of the zone of carbonatite impregnation.

The carbonatite sheets are the result of multiple intrusion comprising both calcitic and dolomitic units. Also late stage veining and hydrothermal alteration has affected the carbonatite. The slabs and large blocks of country rock engulfed by the carbonatite magma are variably to strongly fenitised.

The economic potential of the carbonatite is linked to accumulations of apatite and multi-element mineralisation with barium, thorium, rare earth elements, uranium and lithium. Niobium and tantalum have elevated concentrations in some of the collected samples, but no mineralisation with economic potential has been located so far.

The ultramafic lamprophyre dykes are commonly less than one metre wide, although a few are wider. They carry very few mantle xenoliths and xenocrysts, but the chemistry of some high-pressure minerals suggest their derivation from the diamond stability field within the mantle. The presently known limited distribution and size of the dykes and the scarcity of mantle xenoliths only support a low to moderate diamond potential.

Introduction

A field visit in 2005 to the surroundings of a stream sediment anomaly led to the discovery of a major carbonatite complex and associated ultramafic lamprophyre dykes (Steenfelt *et al.* 2006). With the objective of acquiring information on the size, structure and economic potential of the new complex, a joint project was established in 2006 between the Geological Survey of Denmark and Greenland and the Bureau of Minerals and Petroleum in Greenland. This report documents the results obtained from fieldwork in 2006 and laboratory studies carried out in 2006 and 2007. All acquired data are stored in GIS format on the enclosed DVD, and the present text describes the investigations conducted and conclusions drawn with regard to the structure and economic potential of the complex.

Background

Carbonatites and ultramafic lamprophyres (UML) are products of melts generated deep within or at the base of the lithospheric mantle. The magmas may reach the surface to form lavas and pyroclastic deposits, otherwise they crystallise at depth to form dykes or large intrusive complexes. The rocks are chemically distinct and may contain concentrations of economically interesting minerals and chemical elements such as diamonds in the ultramafic lamprophyres and niobium, tantalum, rare earth elements, phosphorus, iron, uranium, and thorium in the carbonatites. Both rock types are known from other areas in Greenland (Figure 1), where they have been the target for mineral exploration, particularly the Neoproterozoic Sarfartoq carbonatite complex and UML dykes (Secher & Larsen 1980, see Stendal *et al.* 2004 for further references) and the Jurassic Qaqarssuk carbonatite in the Maniitsoq region (Knudsen 1991). The timing of the emplacement of the carbonatites and alkaline dykes can be related to major episodes of continental break-up (Larsen & Rex 1992).

The data analysis leading to the discovery of the carbonatite and associated UML dykes in the Nuuk region together with investigations undertaken in 2005 are reported in Steenfelt *et al.* (2006). The main achievement besides the field investigations was the determination of the Jurassic age of the carbonatite. Using U-Pb isotope data of a zircon crystal located within a boulder of carbonatitic breccia the age was determined to be 158 ± 2 Ma. The discovery of a new Jurassic complex enlarged the extent of Jurassic carbonatitic volcanism in Greenland considerably.

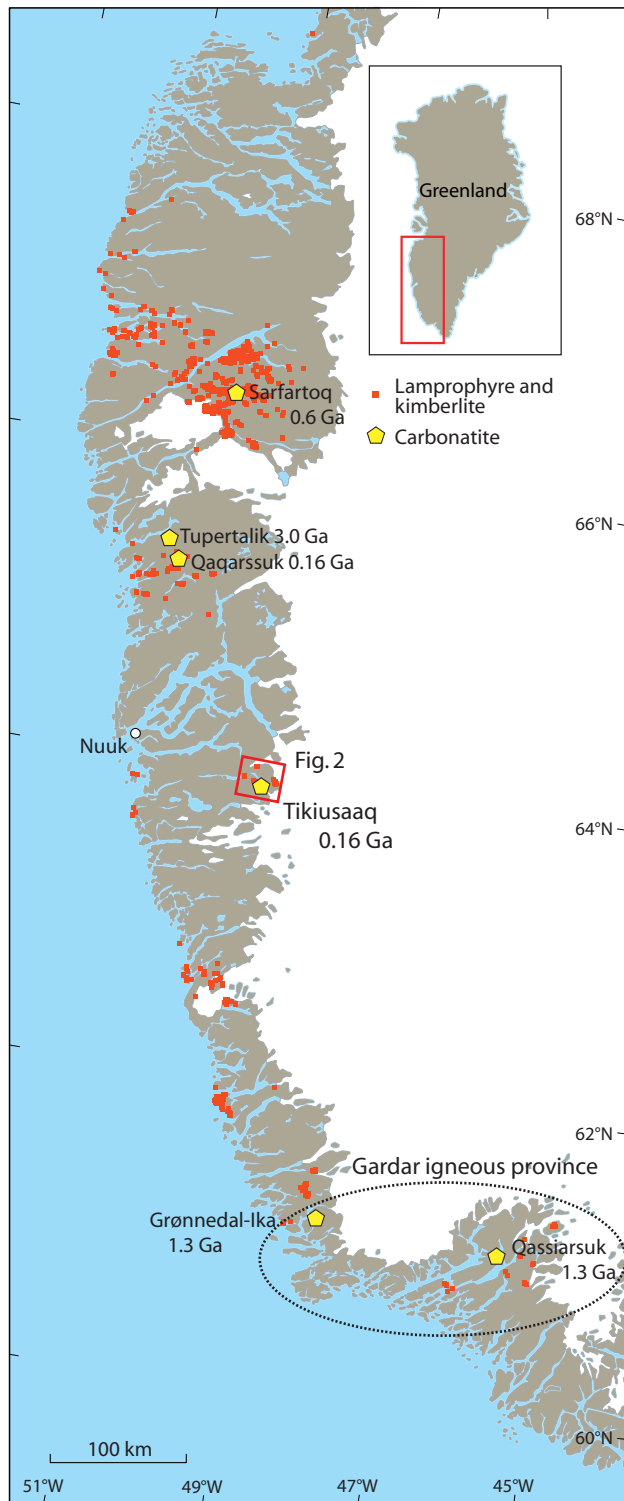


Figure 1. Carbonatite complexes, their names and ages, together with occurrences of lamprophyre and kimberlite dykes in southern West Greenland. Tikiusaaq is located 140 km southeast of capital Nuuk.

Site description and geological setting

The complex, that has been named Tikiusaaq, is situated near the Inland Ice at latitude 64° N in West Greenland, in a hilly area surrounding an elongate depression, which accommodate the lake Isortuarsuk (Figure 2). The lake forms part of the melt water channel in front of a glacier tongue from the Inland Ice. Altitudes vary between 200 m at the lake up to 1100 m above sea level within the area shown in Figure 2. Rocks are well exposed in the higher parts of the terrain, but the lower parts of the hillsides are covered by glacial overburden, till, moraines and glaciofluvial deposits. Vegetation is widespread at low elevation, displayed by red colours in the satellite image (Figure 2), and comprises low and creeping species with local occurrences 0.6 to 2 metres high willow scrubs along streams. The carbonate rich rocks are fertile and vegetation is particularly rich above the carbonatite occurrences.

The carbonatite and ultramafic lamprophyre (UML) dykes are emplaced into Archaean basement comprising tonalitic to granodioritic orthogneisses that enclose and has been deformed together with remnants of supracrustal sequences and anorthosite/leucogabbro. The site of the intrusion lies close to the northern boundary of the Archaean Tasiusarsuaq terrane in a part of Greenland, where there were no previous records of alkaline rock occurrences. Over an area of almost 200 km², the Archaean basement has been fractured and veined as a result of the intrusion of the carbonatitic and associated lamprophyre magmas. The fracturing has influenced later erosion, so that many streams and depressions have a zigzag course reflecting the fracture pattern (Figure 2).

The main occurrence of carbonatite, called the carbonatite core area, was found on the east-facing slope south-east of Isortuarsuk (Figure 3). Massive carbonatite veins or sheets up to ten metres wide and interspersed with chemically altered (finitised) country rock are exposed in five small creeks eroded by streams running across the slope. The lower part of the slope is made up of boulders, gravel and sand derived from the basement and deposited during the retreat of the glacier seen to the southeast. Glacial and post-glacial erosion has formed exposures of rocks and scree on the steep northern creek slopes, while the southern slopes are yielding and covered by soil and vegetation. Thin carbonatite veins have been observed at several localities outside the core area. Large zones of rusty colouration are conspicuous in the landscape surrounding the core area; they reflect fracturing and carbonatite-related coatings of fracture surfaces. Dykes of UML occur outside the carbonatite main occurrence.

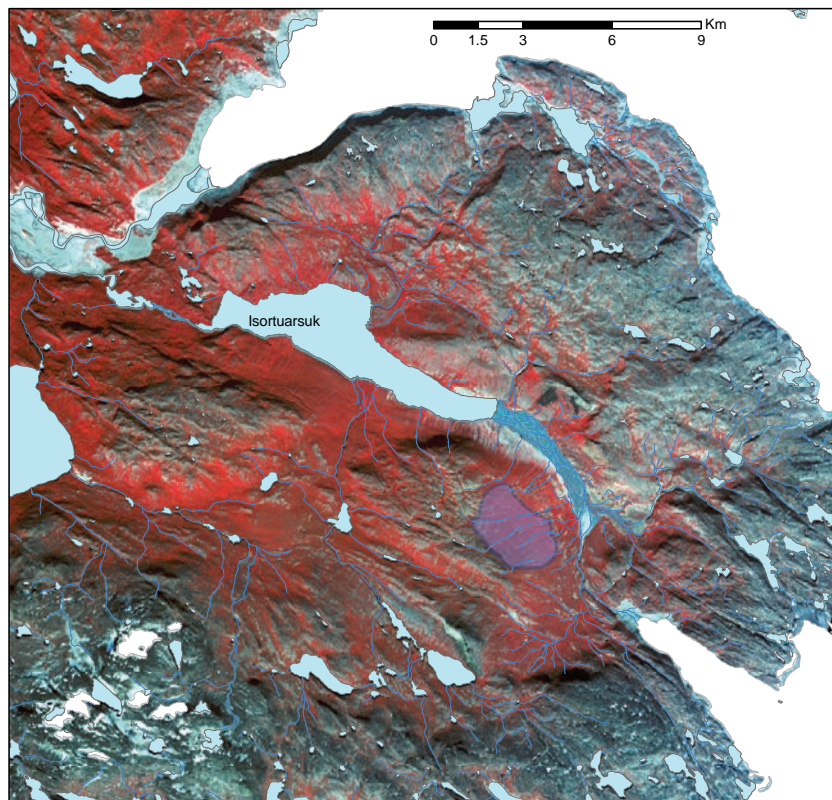
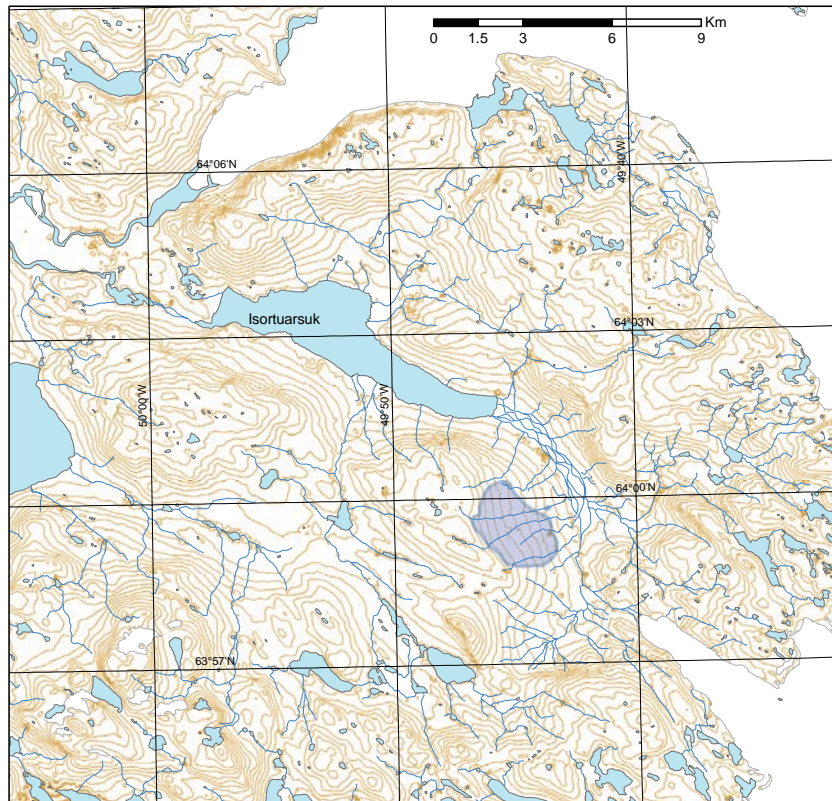


Figure 2. Topographic map and satellite image of the Tikusaaq complex and surroundings. The area where solid carbonatite is exposed in stream creeks is outlined in blue.



Figure 3. *View towards west over the slope where massive sheets of carbonatite are exposed in the stream creeks. The general lack of exposure is evident, and explains why the carbonatite complex has not been discovered in earlier geological reconnaissance and mapping.*



Figure 4. *Typical appearance of scree and occasional outcrops on the northern side of a stream creek and grass and willow scrub lining the sheltered lower parts of the creeks. Buff coloured carbonatite scree at right and far left; dark basement outcrops and scree in between.*

Overview of investigations

This section gives an overview of investigations undertaken in the frame of the project. Details of data acquisition and presentation are provided in the section “Documentation of data on DVD”, and all obtained data are stored on the enclosed DVD.

Field observations

Four geologists participated in fieldwork during the period 10 to 31 July 2006: Agnete Steenfelt, Karsten Secher and Karina Sand from GEUS, Sebastian Tappe from University of Alberta, Canada. The field team was based at a camp centrally in the area with main carbonatite exposures. Two persons spent one week of the field period at a camp near the main occurrences of UML in the north-eastern part of the area. Julie Hollis, working with GEUS geological mapping, supplied information and photographs from the northern part of the area affected by the carbonatite.

The fieldwork comprised three main activities: 1) to visit, describe and sample all exposures of carbonatite and UML with particular attention to evidence for economic mineralisation; 2) to map the carbonatite core area by means of gamma-spectrometric measurements and 3) to carry out mineral exploration. The latter activity comprised sampling of stream sediment and overburden in addition to a search for sites with elevated radioactivity. Experience from the other large carbonatite complexes in Greenland suggests that high gamma-radiation reflects the presence of pyrochlore (uranium-bearing niobium-mineral) or rare earth element (REE) minerals (commonly thorium-bearing).

All observations, photographs and data recorded during the fieldwork are documented on the DVD (see section on data documentation), and they form the basis for the interpretation of the geology.

The field observations are used to illustrate the distribution of the rock types in outcrops and subcrops, i.e. sites where scree or overburden contains abundant fragments of a particular rock type, so that it can be assumed that the rock is present below the cover. Plotting this information on a map illustrates the spatial distribution of rock types and that has been used as input to the geological map.

Measurement of gamma-radiation

Two portable gamma-spectrometers were used qualitatively to find hot-spots and quantitatively to determine equivalent concentrations of U, Th and K at the surface, both in outcrops and in overburden (Figure 5). After a few days of reconnaissance and profiling, it was recognised that the carbonatite has a significantly higher rate of gamma-radiation than the basement and glaciofluvial deposits, and that the radiation measured on top of the overburden could be used to roughly estimate the amount of carbonatite fragments in the overburden. Consequently systematic measurements were made along the creeks as well as

on top of the overburden between exposed parts of the creeks and over the slope between creeks.



Figure 5. Gamma-spectrometric measurements with 20 metres spacing in parallel profiles across slope with overburden containing abundant fragments of carbonatite.

Sampling

Four types of samples were collected. Samples of main *rock* types and of rocks with signs of alteration and mineralisation were collected for chemical analysis and mineral identification. Samples of *stream sediment* were collected to provide information on the mineral potential. Samples of overburden (samples of *soil* beneath vegetation) were collected in one of the gamma-spectrometry profiles to document the chemical composition of the overburden. Samples of *scree* were collected as composite samples representative of exposed rock/scree sections of the creek slopes. Finally samples of gravel (also including sand and silt fractions and therefore termed *soil*) were collected at “hot spots” for chemical analysis and mineral identification. Location and descriptions of samples are stored on the DVD.

Processing of remotely sensed data

Aeromagnetic data from a fixed-wing regional survey and hyperspectral data recorded from satellite (ASTER system) have been acquired and studied with regard to features related to

the carbonatite complex. The aeromagnetic data exhibit a strong positive magnetic anomaly reflecting concentrations of magnetite within the carbonatite.

The satellite data have been used 1) to produce a false-colour image of the terrain useful as a background map, 2) to extract digital landscape data including a terrain model, elevation contours, stream courses and lakes, and 3) to process the hyperspectral data to identify pixels with calcium and magnesium carbonate signature.

Chemistry and mineralogy

A number of 84 rock samples and 55 surface samples (stream sediment, soil and scree) have been analysed, and 60 thin sections of rock samples have been studied under microscope.

Isotope chemistry and age dating

Zircon from one sample of carbonatite and perovskite from three samples of UML have been analysed and their ages determined from the U-Pb isotopic compositions. This work was done at University of Alberta in the laboratory headed by Dr. Larry Heaman.

Studies of kimberlite indicator minerals

Three big samples of UML and one of brecciating carbonatite (two of which were collected in 2005), were submitted for identification of high-pressure mineral phases (kimberlite indicator minerals, KIM) at Overburden Drilling Management Ltd., Ontario, Canada. Returned minerals were probed for their chemical composition. The results were used to estimate the diamond potential using known discrimination diagrams. The clinopyroxene composition was used to establish if the depth of origin was within the diamond stability field.

Documentation of data on DVD

Stored information

The DVD contains documents and data. Documents include this report and an article published in GEUS Bulletin 10 with results obtained 2005 (Steenfelt *et al.* 2006). Data comprise all digital data acquired during the project, i.e. field observations and measurements, sample registration and description, chemical analyses, and satellite hyperspectral data. The spatial distribution of observed and processed data is presented in an ESRI ArcMap project. The data themselves are contained in the attribute files of the ArcMap project, supplemented by EXCEL spreadsheets. Users without an ArcGis license may view, copy and export data by means of ArcReader, which may be downloaded and installed from www.esri.com or from the DVD. Note that the instalment requires 350 MB memory space.

The ArcMap project presents data in a number of grouped layers as described below (Figure 6). Projection parameters are WGS84 as datum and UTM zone 22N as projection method.


- ☐  **Tikiusaaq**
 - ☑ Geographical net
 - ☐ Lakes
 - ☐ Streams
 - ☐ Ice
 - ☐ Field observations
 - ☐ Gamma spectrometry
 - ☑ Geology
 - ☐ Mineralogy
 - ☐ Geochemistry
 - ☐ Terrain model
 - ☑ Remote sensing

Figure 6. *Upper levels of hierarchically arranged layers of the ArcGis project on the DVD accompanying this report. Most of the groups shown here contain several layers as described in the text.*

The lowermost layer group, *Remote sensing*, contains a satellite image and an aeromagnetic image, either of which may serve as a suitable background for the display of point observations. An alternative background is the digital elevation model with elevation curves found in the group *Terrain model*. The uppermost layers comprise topographic features that are useful to superpose on the information, i.e. area-frame, geographical net (longitude and latitude), streams, lakes and ice. The layers are described from top to bottom as they appear in the list of content in the ArcGis project.

Navigation is done using the zoom and pan buttons and mouse. Two fixed view scales are provided by means of bookmarks in the View-menu, one full view, and one close-up of the 'carbonatite core area', where most of the data points are located. Layers can be activated and deactivated from the list of content in the left side of the view.

Description of ArcMap groups and layers

This section describes how the data were acquired, processed and are presented. Comments on the distribution patterns and their significance are given in other sections of this report.

Streams

The stream pattern is drawn from the satellite image.

Lakes

The lakes are drawn from the satellite image.

Ice

This layer displays perennial ice cover, i.e. local ice caps and the Inland Ice.

Geographical net and area frame

The Tikiusaaq complex lies within the frame used in this presentation. The limitation is from 50°10' W to 49°30' W and from 63°54' N to 64°09' N. The net lines represent 10' longitudinal and 03' latitudinal intervals.

Field observations

The group contains three subgroups, *PhotoDescription*, *SampleDescription* and *Locality-Description*. The subgroups contain information related to the visited field localities. The descriptions are accessible using the info button or the attribute tables of the layers. In addition, the descriptions are stored in Excel spreadsheets.

PhotoDescription: The layer displays the positions of field photographs, and the descriptions of their subjects appear in the attribute table. Each photograph position is hyperlinked to the actual photograph(s), which are stored in a separate folder. When the hyperlink button is activated, the symbols change colour and the link is activated by pressing the left mouse-button at the position. Photographs' ID numbers contain information on the year and photographer, e.g. P2006ast0010, and the record for each photo also contains a reference to the field locality where more information about the site may be found.

SampleDescription: The layer displays the distribution of the four types of samples, i.e. rock, stream sediment, soil and scree, collected during the 2006 fieldwork. The attribute table contains a short description of the sample or sample site and a reference to the field locality.

LocalityDescription: The layer displays the positions for field observations. The observed features are described in the attribute table and may be read using the info button. The locality ID number, e.g. 2006ast120, contains the year and geologist. The descriptions are drawn from spreadsheets, where the field notes from each locality are stored. Due to limitations in the size of the text fields in the attribute tables, the descriptions have been split into two columns (Site_descript_1, Site_descript-2).

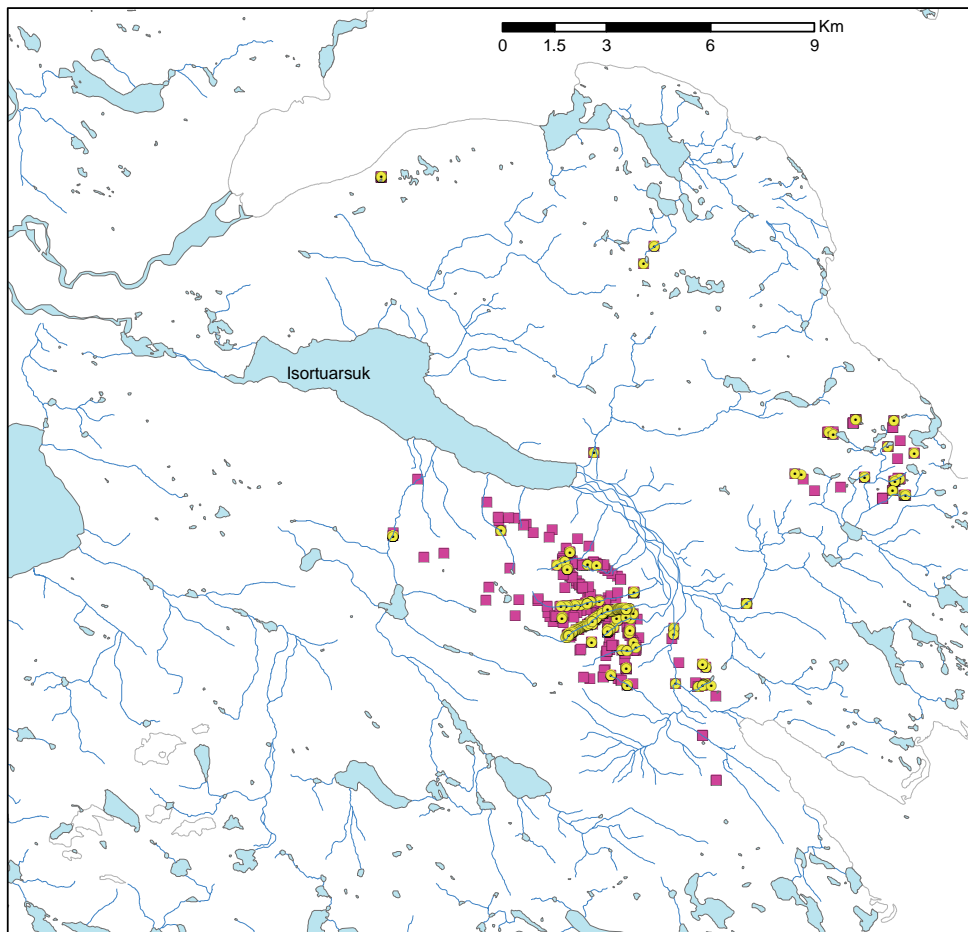


Figure 7. *Distribution of sites described during field work 2006 in the Tikiusaaq complex and surroundings (purple symbols) together with sites where photographs were taken (yellow symbols). All photograph images are stored on the DVD, where they are hot-linked to the photography sites in the ArcMap project.*

Gamma-spectrometry

Data acquisition

Gamma-spectrometric measurements were carried out using two identical portable gamma-spectrometers of the type Gamma Surveyor® from GF instruments Ltd. The spectrometer has a control and data storage unit attached to a lead-insulated, tellurium-activated, sodium iodide crystal detector with a volume of 0.1 litres.



Figure 8. Close-up of Gamma surveyor, the portable gamma-spectrometer used to locate spots of elevated radioactivity and to systematically measure variations in total gamma-radiation as well as in equivalent concentrations of potassium, thorium and uranium. Upper photograph shows the orange lead-insulated detector box with black combined data monitor and control unit mounted on top. Lower photograph shows monitor and control unit from above and top of black GPS monitor to the left. The GPS is plugged into the front of the spectrometer unit, where the socket is covered in metallic coloured tape. The display screen shows spectrometer readings.



The manufacturer has ensured that the spectrometer has been calibrated at and internationally approved calibration site, and peak stabilization is made automatically at short intervals by means of a $^{137}\text{Cesium}$ source.

The gamma-spectrometer records total counts per second as well as estimated ground concentration of potassium (K %), equivalent thorium (eTh ppm) and equivalent U (eU ppm). The spectrometer was equipped with a GPS, enabling the position of the measured site to be stored in the memory of the spectrometer along with the readings. Readings were made over 2 minutes (counting time). This was found to be sufficient to get reproducible data in areas of elevated gamma-radiation. In places with low radiation, the number of counts registered in the U and Th channels was too low to be statistically representative and recorded eU and eTh concentrations from such areas are uncertain. However, as the main purpose was to map the distribution of elevated radioactivity, uncertainties at low level are not considered significant. Higher counting times would have made the survey unacceptably time-consuming.

Measurements of the gamma-radiation were made along profiles (c. 20 m interval) following creeks across the slope, and additionally along tie lines and fill-in points between the profiles at variable intervals. For two creeks, one profile was laid out along the creek bottom and another along the side of the creek, on top of the overburden, to compare response levels. In total, 968 spectral measurements were made (Figure 9).

Data presentation

The group *Gamma-spectrometry* in the ArcGis project has three subgroups reflecting three kinds of data presentation: surface property of measured sites, gamma-spectrometer readings, and images of contoured grids. The file *gam_spec_final.xls* is the basis for the shape files illustrating the recorded data. Each measured point is registered by a profile name and a station number (a profile starting at 0 and continuing at intervals of 20), coordinates, elevation, code for the surface type, spectrometer readings of total counts per second, and equivalent concentrations of K, Th and U.

Surface data: The layer displays the character of the surface at each measuring position. The main surface classes are vegetation, overburden, subcrop and outcrop (Figure 12 and A1 in appendix). The latter two have been further specified according to the lithology into carbonate, fenite (fenitised basement), basement, basement with carbonatite related veining and staining, late breccia, lamprophyre dyke, lamprophyre float, and dolerite dyke. The sites of gamma-spectrometer measurements are not recorded as geological localities, so that more detailed information on these sites is not available. However, a number of field localities have been established close to the measures profiles, see the layer Field Observations.

Gamma readings: The layer displays the variation in readings for the four measured parameters plus the ratio of eU/eTh. Five classes have been used for the size of the symbols based on the frequency distribution (Figure 9).

Contoured grid images: Grids of *Total radiation*, K, eTh, eU and eU/eTh were produced using all measurements made on overburden (called till, surface class 2). These sites are

displayed by the layer "Measured till sites". The gridding was done using the minimum curvature method provided by Geosoft Inc. software. A cell size of 50 x 50 metres and a blanking distance of 100 m were used in the gridding procedure. Contoured grid images together with their legends were imported into ArcGis as georeferenced tif-files.

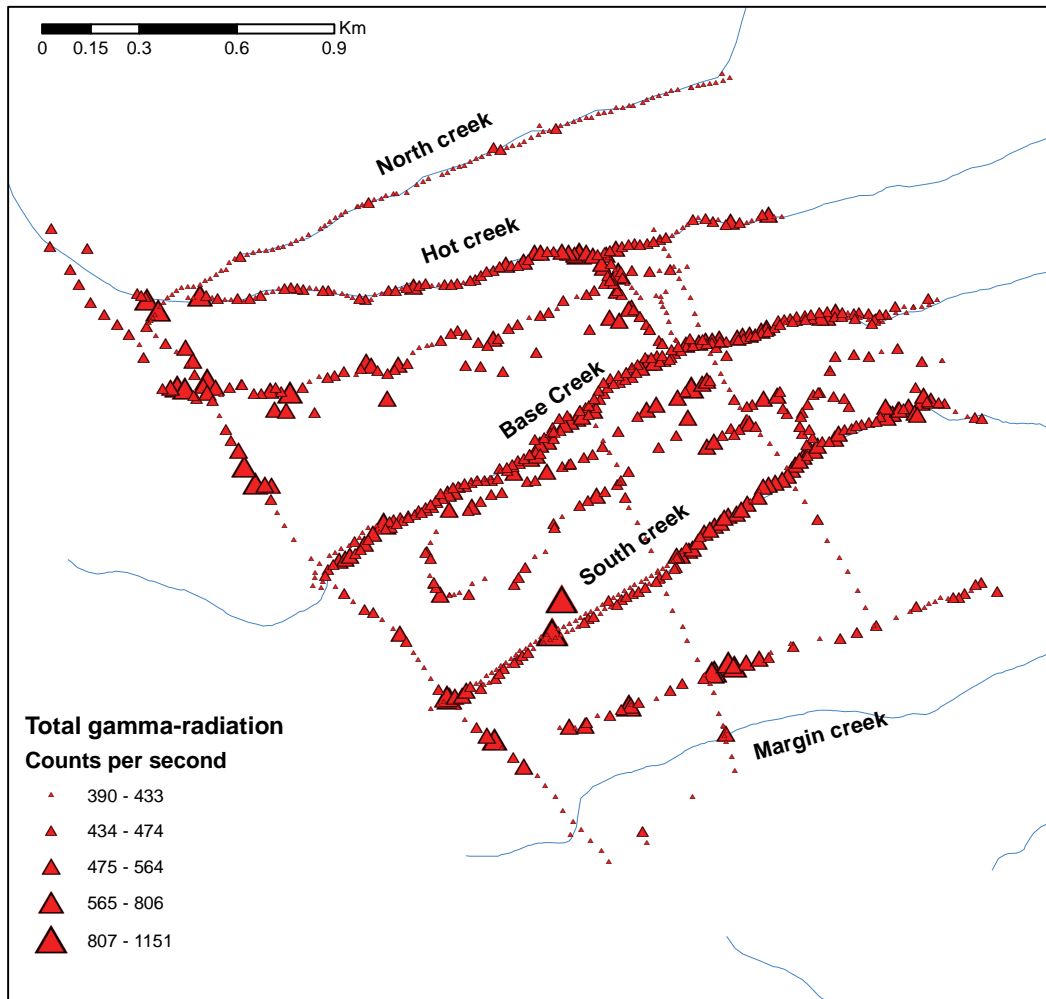


Figure 9. Example of display of ArcGis layer Gamma readings. Variation in total gamma-radiation from gamma-spectrometric point measurements in the area with massive carbonatite.

Geology

The group contains layers presenting data with relevance to the occurrence of carbonatite ultramafic lamprophyres and features related to the emplacement of the carbonatite complex. There are four kinds of data: field observations, interpretation of gamma-spectrometric measurements, features derived from interpretation of remote sensing data, and features interpreting all acquired data.

Field observations

The layer *Surface data all sites* presents the surface-type information given to all field localities and all gamma-spectrometry sites (Figure 10). For the sake of completion, the shapefile includes localities visited in 2005 during GEUS investigations. From the same shapefile, sites with carbonatite as outcrop or subcrop (including scree), i.e. classes 3 and 5, have been extracted to form the layer *Carbonatite sites*. Sites where ultramafic lamprophyre or other dyke associated with the carbonatite complex have been registered in situ or as float (classes 10 and 11) are presented in the layer *Ultramafic lamprophyre* (Figure 10). Sites where alteration related to carbonatite intrusion, i.e. fenitisation of country rock, fracturing and impregnation with carbonatite veinlets (classes 4, 6 and 8) are extracted in the layer *Veining and alteration* (Figure 11). Figure 12 illustrates the lithological classification in the core area.

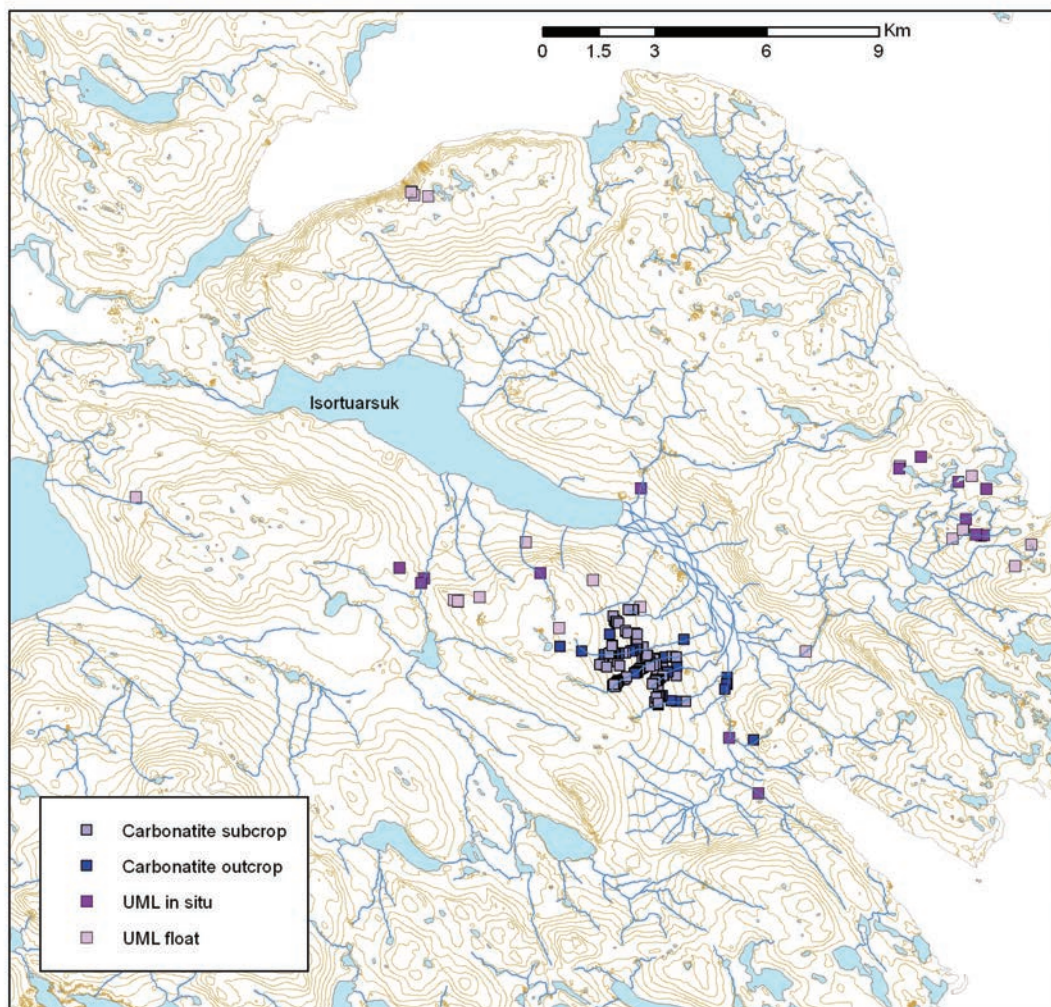


Figure 10. Distribution of sites with outcropping and subcropping carbonatite, and with ultramafic lamprophyre (UML) dykes observed in situ or as transported blocks (float).

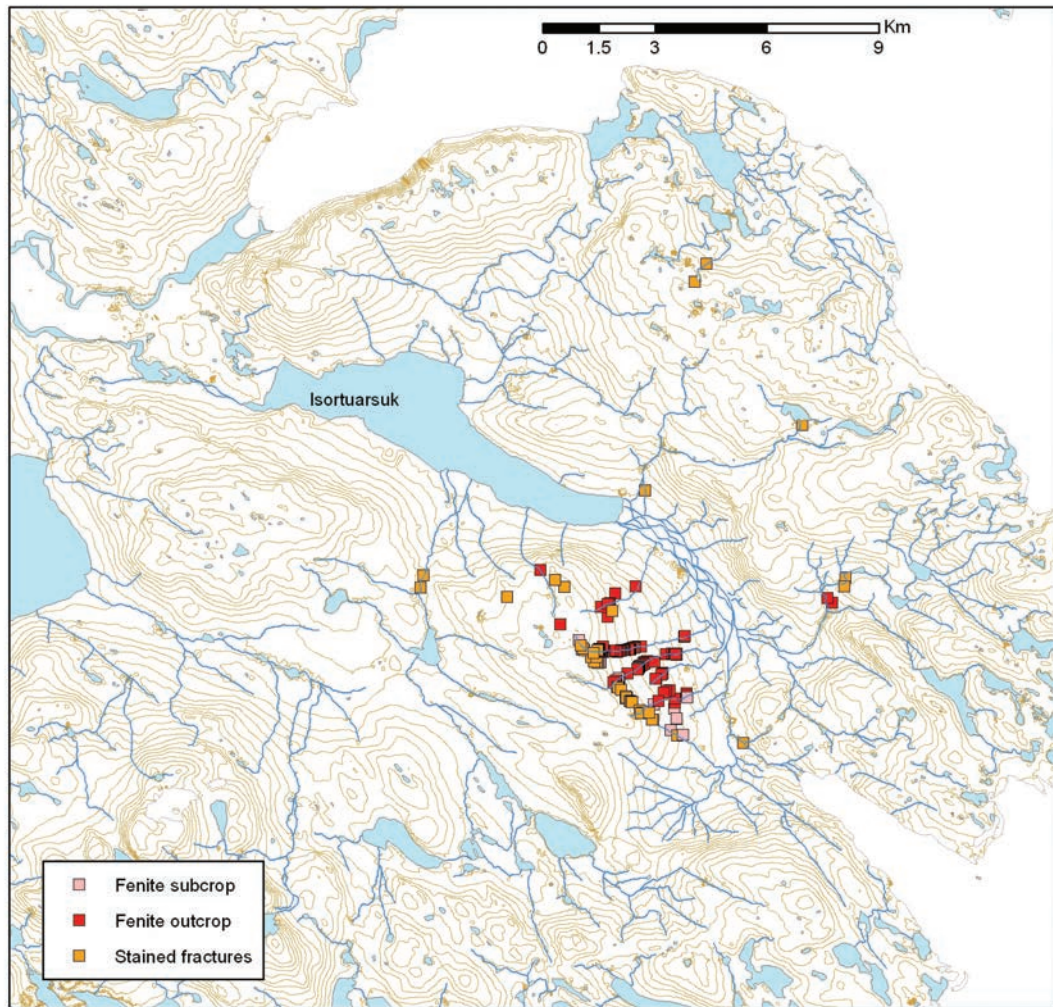


Figure 11. *Distribution of sites where country rock has been tectonically disturbed, veined and chemically affected by the intrusion of carbonatite.*

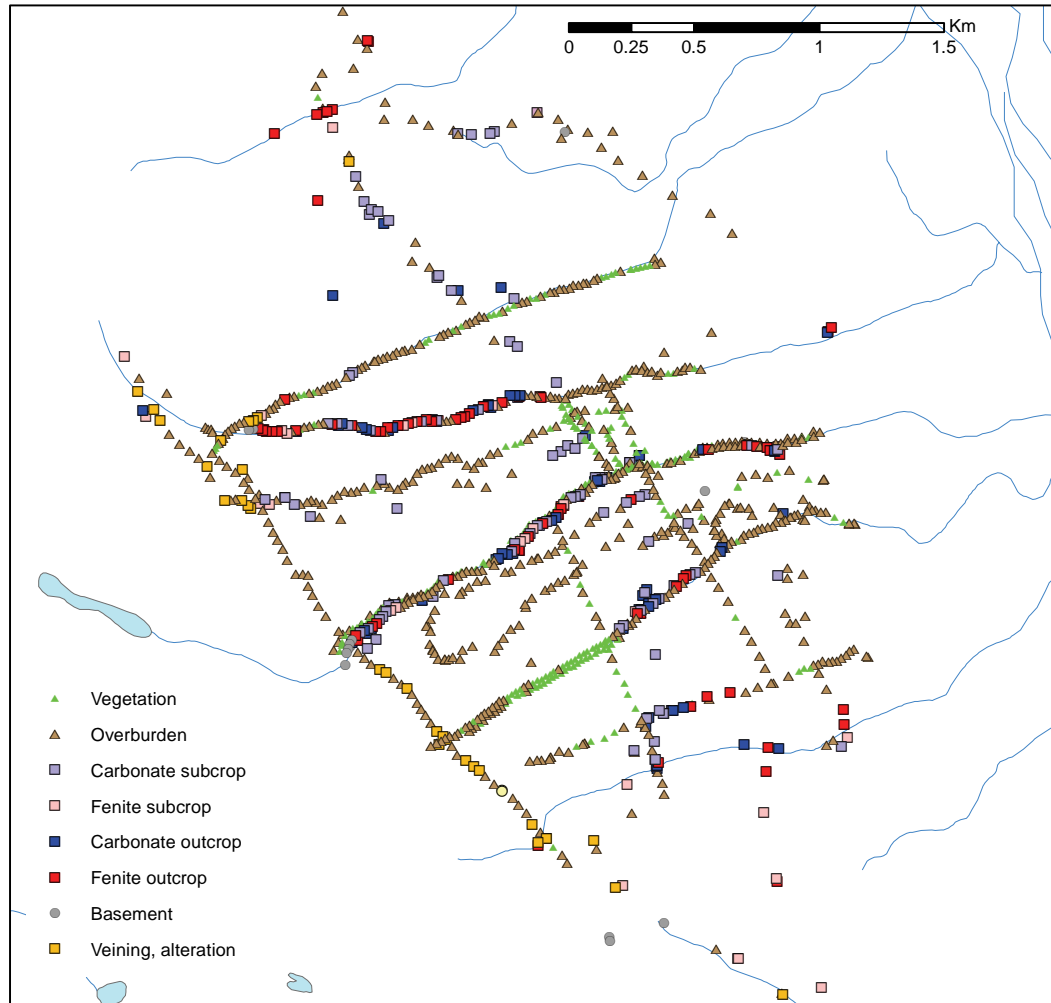


Figure 12. *Lithology of carbonatite core area.*

Results of gamma-spectrometry

The layer, called *eTh window*, shows the distribution of sites with elevated eTh values, defined as the range from 30 to 80 ppm eTh. This range of values were obtained from outcropping carbonatite or overburden with abundant carbonatite fragments and are believed to reflect the presence of carbonatite below scree and overburden. Very high Th values are not included as they reflect mineralisation rather than the carbonatite itself.

Interpretation of remote sensing data

The remote sensing data comprise hyperspectral (ASTER) satellite data and aeromagnetic survey data (see layer description on remote sensing for more documentation on both data sets). In this layer group, the data area used to identify features related to the carbonatite. The ASTER image has been used as a basis for drawing topographical lineaments and to map pixels with calcite and dolomite spectral signature, respectively. The aeromagnetic image has been used to draw magnetic lineaments and the outline of an aeromagnetic anomaly created by the magnetite within the carbonatite. The magnetic anomaly outline

has been divided arbitrarily into two zones, the core with values roughly above 220 nanotesla and rim with values between 70 and 220 nanotesla.

Interpretation of all acquired data

Two features area drawn based on the distribution of phenomena attributable to the emplacement of the carbonatite and associated dykes. The carbonatite core encloses data points believed to reflect massive sheets of carbonatite, i.e. outcrops, scree, overburden with abundant carbonatite pebble, elevated eTh concentrations, ASTER pixels with dolomite or calcite. The carbonatite core thus represents the area where the massive carbonatite sheets occur at the surface or directly below the overburden. The carbonatite complex outline encloses all known occurrences of carbonatite dykes and veins, fenitised basement, carbonatite-related jointing and staining of joint surfaces, ultramafic lamprophyre dykes (in situ), and most ASTER pixels with calcite or dolomite signature outside the carbonatite core. Calcite pixels on the western and south-western side of the complex outline have not been included because there are no field observations to sustain the presence of carbonatite material in that area.

Mineralogy

The layer Mineralogical data displays the distribution of rock samples with mineralogical data derived from examination of thin sections. The attribute table contains the minerals identified and their abundance, i.e. major or minor constituent. The layer Apatite shows where apatite has been identified. Users with ArcMap license may use the symbology tools to plot occurrences of other minerals.

Geochemistry

The layer group presents the results of chemical analyses of rock and surface samples, the latter comprising samples of stream sediment, soil and scree. Two aspects are considered: 1) main features of the geochemistry of common rock types within the carbonatite complex and ultramafic lamprophyres, and 2) the distribution of samples with high concentrations of chemical elements of economic interest.

Data acquisition

Rock samples have been crushed, milled and analysed at ACME Analytical Laboratories Ltd. Most rock samples were analysed by packages 4A, 4B and 1DX (see Table 1 for information on analytical packages). Surface samples have been dried and screened at GEUS and the < 0.1 mm grain size fractions have been analysed at ACME. The surface samples plus seven radioactive or otherwise mineralised rock samples were analysed by packages 7TX and 5A. The original analytical data as received from the laboratory are included in the files stored in the folder LabData. These files contain information on detection limits and comments on methods. Table 1 lists elements and components determined and documentation on the packages.

Package	7TX	5A		4A	4B	1DX
Method	ICP-MS/ES	INA		ICP-ES	ICP-MS	ICP-MS
Sample type	SS+minRO	SS+minRO		RO	RO	RO
ArcMap Layer	Mineralisation			Rock chemistry		
LOI				LOI		
CO2				CO2		
Ag	Ag	Ag				Ag
Al	Al			Al2O3		
As	As	As		CaO		As
Au		Au				Au
Ba	Ba	Ba			Ba	
Be	Be				Be	
Bi	Bi					Bi
Br		Br				
Ca	Ca	Ca				
Cd	Cd					Cd
Co	Co	Co			Co	
Cr	Cr	Cr		Cr2O3		
Cs		Cs			Cs	
Cu	Cu					Cu
Fe	Fe	Fe		Fe2O3		
Ga					Ga	
Hf	Hf	Hf			Hf	
Hg		Hg				Hg
Ir		Ir				
K	K			K2O		
Li	Li					
Mg	Mg			MgO		
Mn	Mn			MnO		
Mo	Mo	Mo				Mo
Na	Na	Na		Na2O		
Nb	Nb				Nb	
Ni		Ni		Ni		Ni
P	P			P2O5		
Pb	Pb					Pb
Rb	Rb	Rb			Rb	

Package	7TX	5A		4A	4B	1DX
Method	ICP-MS/ES	INA		ICP-ES	ICP-MS	ICP-MS
Sample type	SS+minRO	SS+minRO		RO	RO	RO
ArcMap Layer	Mineralisation			Rock chemistry		
S						S*
Sb	Sb	Sb				Sb
Sc	Sc	Sc		Sc		
Se		Se				Se
Si				SiO2		
Sn	Sn	Sn			Sn	
Sr	Sr	Sr			Sr	
Ta	Ta	Ta			Ta	
Th	Th	Th			Th	
Ti	Ti			TiO2		
Tl						Tl
U	U	U			U	
V	V				V	
W	W	W			W	
Y	Y				Y	
Zn	Zn	Zn				Zn
Zr	Zr				Zr	
La		La			La	
Ce	Ce	Ce			Ce	
Pr					Pr	
Nd		Nd			Nd	
Sm		Sm			Sm	
Eu		Eu			Eu	
Gd					Gd	
Tb		Tb			Tb	
Dy					Dy	
Ho					Ho	
Er					Er	
Tm					Tm	
Yb		Yb			Yb	
Lu		Lu			Lu	

*S not determined in rock samples with sample ID beginning with 488

4A: 0.200 g sample by LiBO₂/Li₂B₄O₇ fusion, dilute nitric acid digestion, analysis by inductively coupled plasma emission spectrometry (ICP-ES).

4B: 0.200 g sample by LiBO₂/Li₂B₄O₇ fusion, analysis by inductively coupled plasma mass spectrometry (ICP-MS).

1DX: 0.50 g sample leached with 3 ml 2-2-2 HCL-HNO₃-H₂O at 95° C for one hour, diluted to 10 ml, analysed by inductively coupled plasma mass spectrometry (ICP-MS).

7TX: 0.500 g sample, 4 acid (HF-HClO₄-HNO₃-HCl) digestion to 100 ml, analysis by inductively coupled plasma emission spectrometry or mass spectrometry (ICP-ES/ICP-MS).

5A (BQ-NAA-1): 5 g sample analysed by instrumental neutron activation (INA). Detection limits are elevated in samples with high REE's and/or low sample weight. Results in extreme cases should be taken as semi-quantitative.

Table 1. Elements and oxides determined in analytical packages provided by ACME analytical Laboratories Ltd. Analytical results are stored in the folder LabData on the DVD. SS: Surface samples. RO: Rock samples. minRO: mineralised rock samples. Elements in bold characters are included in the ArcGis shapefiles on the DVD.

Data presentation

Rock chemistry. The layer shows the spatial distribution of six components, three major element oxides and three trace elements, which are typically enriched in carbonatitic rocks and lamprophyres. A five-class scale of symbols, increasing in size with concentration, is used for each component to illustrate the compositional variation.

Mineralisation. The layer displays the distribution of concentrations of 10 elements in rock and surface samples. The surface samples (triangular symbols) include all collected samples, while the mineralised rock samples (square symbols) comprise seven samples collected as mineralised, plus nine from the remaining rock samples with anomalously high values of one or more of the 10 elements. The sub-layers are arranged in alphabetical element order, each element having an individual colour. A three-class scale of symbols illustrates the compositional variation.

In the attribute table the digit 0 comprises values not determined as well as values below detection limit. The determined values and detection limits are available in the original laboratory files in the folder LabData on the DVD.

Terrain model

The group contains two layers derived from processing of data acquired by ASTER satellite imagery (see below for data acquisition).

The *digital elevation model* is presented as a grey-scale grid image with a grid cell size of 15 metres. The model has not been finally corrected for errors so that grid cells with false values (low or even negative values) still occur locally, particularly in stream valleys and around lakes.

Elevation contours extracted from the digital elevation model are given at 50 metres elevation interval. Owing to the errors just mentioned, the contour pattern is locally erroneously complicated. It has not been attempted to correct such errors in this presentation, as the purpose of showing the contours is illustration rather than documentation. The elevation values may be read off the contour lines using the info-button.

Remote sensing

Aeromagnetic image

The contoured grid image of aeromagnetic data is a small part of a grid image of the total magnetic field derived from the survey 'Aeromag 1998' conducted by Sander geophysics Ltd. and jointly financed by GEUS and BMP. The survey was flown at a terrain clearance of 300 metres (draped) in regular north-south lines spaced 500 metres with east-west tie-

lines spaced 5000 metres. The gridding and imaging of the measured total field has been made using software from Geosoft Inc. The aeromagnetic map of entire southern West Greenland and more information on the data may be found at the GEUS website under 'Products/Services'.

Satellite image

The area is covered by a subset of ASTER (Advanced Spaceborne Thermal Emission and Reflection Radiometer) satellite image (nominal scene:

AST_L1B_003_08252000150959_06232003073537) obtained from Eros Data Centre, USA. The "at sensor" radiance data are registered in UTM projection (Zone 22, Datum WGS 84). The spatial resolution of the Aster VNIR (visible and near-infrared, 3 bands) and SWIR (short wave infrared, 6 bands) data is 15 and 30 metres, respectively. The SWIR data were corrected for "sensor crosstalk" and the VNIR and SWIR data were co-registered to the 15 m resolution. An atmospheric correction has been applied to the VNIR and SWIR data, whereby the radiance data were transformed to surface reflectance data.

The ASTER image (Figure 13) is a colour composite (RGB) of VNIR bands 3 (red), 2(green) and 1 (blue). The mapping was based on the SAM (spectral angle mapper) algorithm.

The ASTER data were processed to identify pixels with dolomite or calcite spectral signatures. The carbonate spectra from the USGS mineral spectral library were used as reference. The result is presented in the Geology layer group (Figure 13).

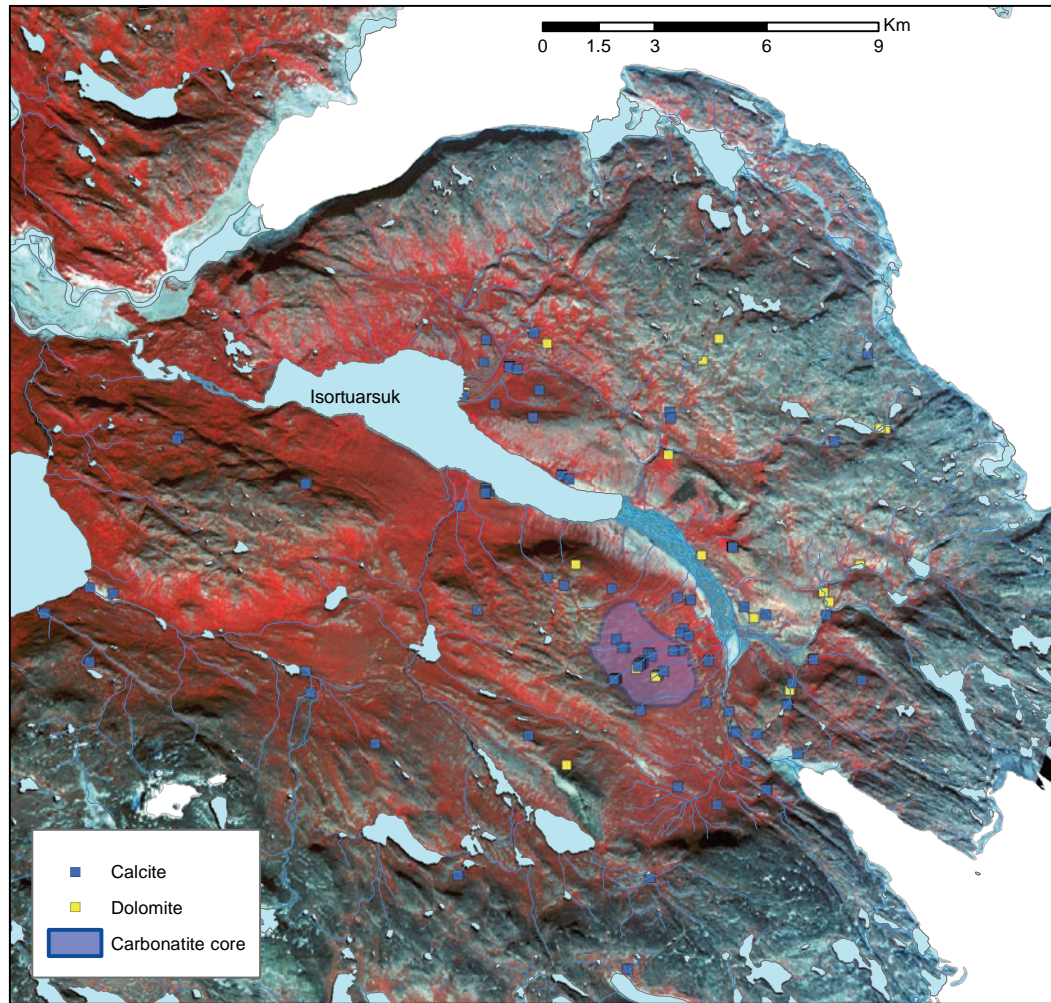


Figure 13. *Three-band image and result of processing of ASTER spaceborne data. Symbols mark points where pixels containing hyperspectral signatures from calcite (light green symbols) and dolomite (yellow symbols) were identified. Red colours reflect vegetation, grey colours largely reflect exposed rock surfaces. The south-westernmost calcite sites indicated by the hyperspectral data have not been covered by field work, and thus can not be related to the carbonatite with certainty.*

Results

Gamma-spectrometry

In addition to the presentation on DVD, where recorded values are shown as point data and grid images, diagrams have been constructed to illustrate the variation in lithology and gamma-radiation along the profiles and in relation to the terrain. The distribution patterns of the radioactive elements, displayed by the grid images, are also discussed in this section.

Lithological and gamma-spectrometric profiling

Along each of the main profiles, the lithology and gamma-spectrometric readings were recorded at 20 m interval. The resulting data is shown in diagrams in the appendix. They are constructed by plotting lithology as symbols in an elevation-longitude space and gamma-spectrometric data against their longitude using lithology symbols. The main impression gained by studying the profiles is that the gamma-radiation varies considerably within and between lithological units. The profiles illustrate the difference in radiation level between points measured on top of the vegetation and on outcrops or overburden. It should be mentioned that a small part of the variation is probably due to variable geometry of the measured site. Thus, where the gamma-spectrometer is close to one or both walls of the creek, the detector receives radiation from the sides and readings get enhanced.

The profiles also illustrate the generally elevated radiation in sections of the profiles where carbonatite and fenite is common, in contrast to the irregularly distributed single occurrences of 'hot-spots', where either Th or U (or in rare cases both elements) exhibit high values. Most anomalies occur in the upper part of Hot creek and the lower part of South creek.

Gamma-spectrometric mapping

A way to display variation trends between profiles is to construct a grid map. There was not capacity to carry out measurements in a systematic grid, but by means of the available measurements between profiles, it was possible to model a grid. To avoid bias, the gridding was based only on measurements made on overburden. A minimum curvature algorithm was used in the gridding. One of the five grid images produced (Total radiation, K, eTh, eU and eU/eTh ratio) are shown here (Figure 14). A north-west trending anomaly in the centre is taken as reflecting a sheet of carbonatite flanked by a sheet of country rock to the south-west. Anomalies in the upper (south-western) parts of the creeks are due to strong point anomalies.

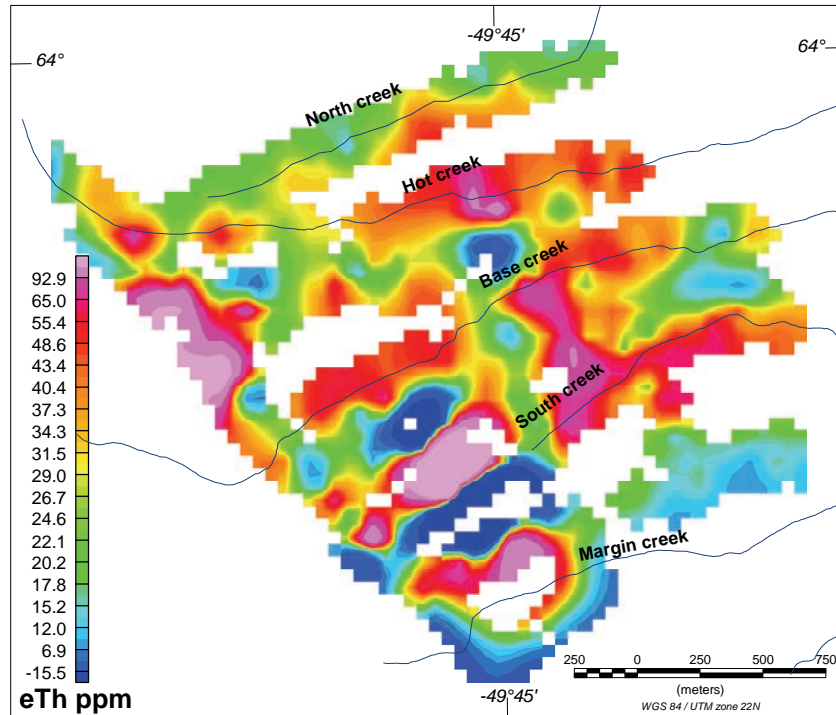


Figure 14. Grid image of equivalent thorium concentrations measured by gamma-spectrometer on sites of overburden.

Structure and components of the Tikiusaaq complex

The fieldwork and study of satellite images have shown that a large area has been affected by fracturing and carbonatite impregnation, while exposures of massive sheets of carbonatite are confined to stream creeks across a gentle slope south-east of Isortuarsuk (Figure 15). Dykes of ultramafic lamprophyre, carbonatite and brecciating carbonatite are formed in associated intrusive events and have a wider distribution than the massive carbonatite.

The large area of carbonate impregnated fractures and the limited exposures of massive carbonatite suggest that massive carbonatite has a wider distribution at depth, so that only a small part of the massive carbonatite is exposed. Also the shape of the magnetic anomaly suggests that the massive carbonatite extends towards the east below glaciogenic deposits and further east below the rocks. The observations are taken to imply that the present exposure represents the roof zone of an intruding carbonatite.

The orientation of the massive carbonatite sheets is difficult to determine, as the sheets can not be connected between the creeks, i.e. they are not exposed in three dimensions. In the creeks, they appear vertical with some variation due to local flow patterns around interspersed sheets or large blocks of country rock, and the layering and sheeting appears to be at a high angle to the creek direction, i.e. WNW to N. The gamma-spectrometric survey

show some elongated NW-trending anomaly patterns giving the same impression (Figure 14).

The pronounced pattern of brittle fractures is believed to be associated with the emplacement of the carbonatite complex (Figure 16). The fractures and joints form a conjugate system, enhanced by topography and directing the course of streams, with directions 50° to 70° and 120° to 140° . The latter is more or less parallel to the preferred WNW strike of fold patterns in the Archaean country rock, and appears to have directed the orientation of massive sheets, or at least of the visible parts of them, and some of the carbonatite dykes NW and SE of the massive carbonatite. Prominent 70° fracturing has directed the orientation of the ultramafic lamprophyres in the north-eastern area (Figure 15).

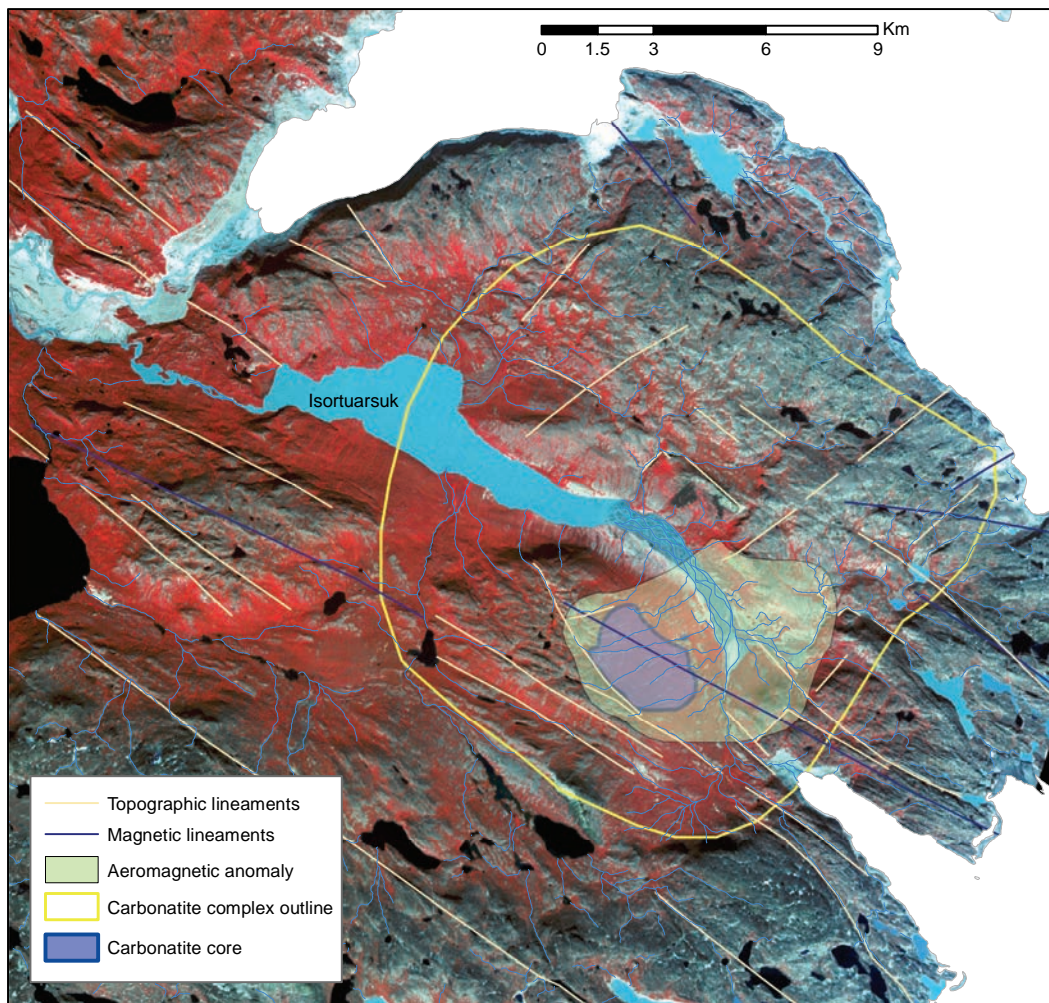


Figure 15. Regional structural pattern indicated by lineaments in topographical and aeromagnetic data and outline of Tikiusaaq complex. Inner shaded figure marks the core area where massive carbonatite sheets are exposed, and large shade outlines the area affected by the intrusion of the carbonatite.



Figure 16. *Strong brittle fracturing and yellow-rusty colouration due to carbonatite veining and impregnation exposed in a stream on the northern side of the alluvial deposits at the eastern end of Isortuarsuk.*

Carbonatite

The massive carbonatite sheets are variable in width, and because many are covered in scree their true widths and structures are not known with certainty. They appear to be up to 10 metres wide, but many are only a few metres. The carbonatite sheets exhibit multiple veining and internal brecciation indicating repeated magma emplacements. Chemical analyses demonstrate that the carbonatite comprise calcitic, dolomitic and ankeritic components, the former two being the most common (Table 2). It was not always possible to distinguish calcitic (sölvite) and dolomitic (rauhaugite) components in the field. The spatial distribution of samples of each rock type shows that they occur together; hence it is likely that they represent individual phases intruded into the same area.

The carbonatite has variable contents of apatite, phlogopite, and magnetite. Other accessory minerals comprise barite, zircon, baddelyite, olivine, alkali amphibole, rutile, iron and zinc sulphides, and chlorite. The chemical analyses conducted within this project indicate that samples with dolomitic composition have the highest contents of phosphorus and niobium.



Figure 17. *One of the main outcrops of carbonatite in Base creek. The massive carbonatite exhibits subvertical flow banding and late brown veins.*

Carbonatite veins occur within and outside the 'core area' with massive sheets and comprise at least two types, beforosite (ankeritic carbonate) and brecciating veins. Beforsite veins are commonly straight, less than 30 cm wide and have brown colours. Some have elevated radioactivity. The brecciating veins are irregular up to 2 metres wide and characterised by abundant rounded and angular inclusions of country rock, fenitised country rock, carbonatite and glimmerite (rock rich in brown mica). The brecciating veins appear to be enriched in Nb and REE (Table 2).

Fenite

The country rock occurring between the carbonatite veins is variably fenitised, i.e. chemically attacked by the carbonatite liquid and volatiles. The fenitisation leads to desilication and alkali enrichment, the latter resulting in formation of albite, bluish-green alkali amphiboles and green aegirine. Also limonite and chlorite are commonly seen in the fenite. The main components of the country rock intruded by the carbonatite are granodioritic gneiss, amphibolite and leucogabbro.



Figure 18. *Large outcrop of moderately fractured and fenitised mafic countryrock in Base creek. Centimetres to decimetres wide veins of pink to buff carbonatite penetrate the fenite.*

Ultramafic lamprophyre

Many of the observed dykes of ultramafic lamprophyre are less than one metre wide and can only be followed over few metres or few tens of metres, and it is difficult to get a good impression of the composition and structure of these dykes. A few are considerably wider, up to 4 metres, and they exhibit flow banding and shearing along margins. Loose blocks are locally abundant on the surface and they are probably not transported very far. The most common rock type is dark grey, unweathered, unfoliated, but fractured and calcite-veined, and strongly magnetic. It consists of fine-grained (0.1 mm) groundmass of calcite with c. 15% magnetite and 3% brown mica (probably talc) with sparse (1%), small (1-2 mm), rounded magnetite and even sparser, similar-sized, fresh, rounded olivine xenocrysts, and phenocrysts of fresh olivine, magnetite and talc. Brown mica (phlogopite or talc) has been seen in some dykes and the amount of calcite and magnetite varies among dykes.

Element	Calcitic carbonatite (13)			Dolomitic carbonatite (13)			Fenite (8)		
	Median	95 perc	Max	Median	95 perc	Max	Median	95 perc	Max
SiO ₂	0.86	2.05	2.25	1.17	5.37	5.97	44.66	60.02	62.37
Al ₂ O ₃	0.17	0.54	0.57	0.30	1.31	1.41	14.13	19.74	21.07
Fe ₂ O ₃	2.10	5.05	5.90	5.06	12.04	18.81	6.62	12.77	15.52
MgO	5.71	7.62	7.87	14.84	17.54	17.86	5.45	16.13	16.34
CaO	47.10	49.60	50.99	31.28	37.04	37.74	7.55	20.67	20.76
Na ₂ O	0.08	0.11	0.11	0.09	0.16	0.16	1.19	5.14	5.59
K ₂ O	0.18	0.52	0.55	0.22	1.27	1.37	5.95	9.72	9.93
TiO ₂	0.03	0.05	0.05	0.03	0.14	0.18	0.22	0.51	0.61
P ₂ O ₅	1.22	4.44	4.99	3.80	9.73	10.84	0.36	4.60	4.79
MnO	0.38	0.59	0.68	0.48	1.07	1.66	0.12	0.40	0.49
LOI	41.50	43.14	43.20	38.60	43.80	44.10	8.10	26.91	33.00
SUM	99.11	99.38	99.48	98.95	99.41	99.42	99.63	99.86	99.88
Ag	0.1	0.1	0.1	0.2	0.2	0.2	0.2	0.2	0.2
As	1	7	8.9	1.1	4.0	4.7	3	40	55
Au	1.6	2.04	2.1	4.5	41.1	43.4	1.8	7.1	8.0
Ba	414	1497	1890	199	8680	19816	1871	4373	5472
Be	1	1.7	2	2	4.8	6	6.0	27.2	30.0
Bi	0.10	0.10	0.10	0.25	0.39	0.40	0.30	0.66	0.70
Cd	0.5	0.98	1.1	0.5	0.82	1	0.1	0.7	0.8
Co	3.5	11.8	12.5	7.8	11.3	12.5	18	28	32
Cr	<7	<7	<7	<7	24	27	55	150	164
Cs	0.1	0.1	0.1	0.1	0.4	0.4	0.5	1.7	1.7
Cu	0.5	3.2	4.7	2.7	14.6	18.9	7	24	29
Ga	2.4	3.58	4.3	2	5.3	6.3	16	23	24
Hf	3.7	6.5	7.2	3	6.8	7.7	2	6	6
Mo	0.3	5.2	6	0.5	11.4	18.6	1	5	6
Nb	9.6	140	206	210	1589	2044	102	264	276
Ni	0.75	2.27	2.9	1.85	9.0	12.5	23	105	130
Pb	4.2	12.8	13.8	4.6	28.3	51.2	10	66	78
Rb	3	14.04	15.3	9.4	32.9	33	102	217	252
Sb	0.25	0.375	0.4	0.25	0.73	0.8	0.4	3.0	3.9
Sc	16	20.8	22	15	20.4	21	17	42	49
Sn	1	2.8	3	1	1.85	2	1.0	5.0	6.0
Sr	7355	20139	21828	6731	9300	9416	957	3743	3760
Ta	1	6.38	6.8	5.8	150	163	2	19	23
Th	3	46	102	8	207	372	47	281	381
Tl	0.1	0.1	0.1	0.1	0.1	0.1	0.1	0.2	0.2
U	0.3	3.16	6.1	5.9	162	169	2	13	16
V	17	55.4	65	13	29.2	32	72	130	143
W	0.2	0.62	0.8	0.4	1.4	1.7	1	3	4
Yt	63	94	109	37	79	94	40	99	100
Zn	12	59.8	106	39	187	379	97	357	430
Zr	6	288	400	9	266	404	83	266	303
La	289	573	615	207	513	759	55	522	619
Ce	722	1252	1300	522	1242	1736	124	1134	1336
Pr	78	122	124	63	137	188	16	110	123
Nd	295	414	427	244	543	694	64	382	422
Sm	40	61	75	35	84	88	21	50	57
Eu	11	19	26	9	21	22	8	16	18
Gd	26	44	61	22	41	47	20	47	55
Tb	3.9	6.4	8.7	2.9	5.6	5.8	2.6	8.6	9.9
Dy	16	25	32	10	21	22	10	32	35
Ho	2.3	3.3	3.9	1.3	2.9	3.3	1.4	3.9	3.9
Er	5.0	7.0	7.1	3.1	6.0	7.4	3.1	6.8	6.8
Tm	0.6	1.0	1.0	0.4	0.7	0.9	0.4	0.7	0.7
Yb	3.5	5.8	6.0	2.0	3.1	4.1	1.8	3.4	4.1
Lu	0.5	0.8	0.8	0.3	0.4	0.5	0.2	0.5	0.6

Table continues

Element	UML (20)			Breccia carbonatite vein (9)		
	Median	95 perc	Max	Median	95 perc	Max
SiO ₂	20.96	31.33	32.47	21.11	32.09	34.39
Al ₂ O ₃	2.75	5.78	6.73	5.15	8.48	9.49
Fe ₂ O ₃	13.40	15.60	17.33	9.54	10.93	11.21
MgO	14.55	23.35	28.01	10.11	11.81	11.94
CaO	18.81	27.45	34.15	20.57	38.75	47.15
Na ₂ O	0.15	2.35	2.38	1.07	2.49	2.74
K ₂ O	1.30	3.51	4.18	3.19	4.09	4.23
TiO ₂	3.61	4.30	4.43	0.30	0.40	0.43
P ₂ O ₅	1.05	2.74	3.06	2.38	2.75	2.79
MnO	0.24	0.37	0.38	0.33	0.51	0.56
LOI	17.95	29.14	33.70	25.00	38.06	42.30
SUM	99.5	99.7	99.7	99.33	99.60	99.64
Ag	0	0	0	0.1	0.3	0.3
As	1.1	2.5	4.0	5	9	11
Au	2.3	4.6	5.9	2.5	4.1	4.7
Ba	1056	2366	2556	682	1817	1874
Be	3.0	7.1	8.0	9.0	33.0	33.0
Bi	0.1	0.2	0.2	0.1	0.1	0.1
Cd	0	0	0	0.4	0.7	0.7
Co	58	94	105	22	26	26
Cr	445	1482	1554	48	111	137
Cs	1	2	2	1.0	2.8	3.0
Cu	97	121	125	15	26	26
Ga	11	16	17	11	16	16
Hf	13	23	24	9	16	18
Mo	0	1	8	1	2	2
Nb	230	583	647	627	1139	1357
Ni	156	846	971	19	53	67
Pb	6	17	19	19	27	30
Rb	52	101	104	87	103	104
Sb	0	0	0	0.3	1.4	1.8
Sc	23.0	33.1	35.0	25	40	44
Sn	3	5	6	3.5	6.7	7.0
Sr	2286	3997	4940	2474	4946	6012
Ta	12	21	23	13	19	21
Th	24	145	257	64	135	149
Tl	0	0	0	0.2	0.4	0.4
U	5	23	31	21	32	36
V	199	322	351	110	121	124
W	1	21	43	2	11	15
Yt	32	64	77	59	77	84
Zn	97	153	163	137	168	168
Zr	541	1003	1023	330	719	824
La	190	482	521	402	1196	1685
Ce	437	1092	1159	901	2358	3250
Pr	45	112	115	92	203	275
Nd	165	415	416	312	651	855
Sm	23	46	51	38	63	76
Eu	6	12	13	10	15	18
Gd	15	28	32	22	32	35
Tb	2	4	4	3.4	4.3	4.7
Dy	8	17	18	14	17	17
Ho	1.1	2.3	2.8	2.0	2.6	2.8
Er	2.6	5.3	7.0	5.2	6.3	6.8
Tm	0.4	0.9	1.0	0.8	0.9	0.9
Yb	2.1	5.7	6.2	4.4	5.2	5.3
Lu	0.3	0.9	1.0	0.6	0.7	0.7

Table 2. (continued). Summary statistical parameters for the chemistry of major rock types of the Tikiusaaq complex. Number of samples in parentheses. 95 perc: 95th percentile. Max: Maximum



Figure 19. *Ultramafic lamprophyre dyke intruding granulite facies orthogneiss in the north-eastern part of the Tikiusaaq complex.*



Figure 20. *Block of ultramafic lamprophyre with conspicuous phenocrysts of olivine and magnetite, and orthogneiss fragments.*

The picking results are given in the table below. One sample of UML (459118) did not have any kimberlite indicator minerals, whereas the other samples returned a few grains of garnet and chrome diopside in the finer of the three grain size fractions, and many grains of ilmenite and olivine in all fractions (Table 3).

Sample ID	1.0-2.0 mm						0.5-1.0 mm						0.25-0.5 mm					
	GP	GO	DC	IM	CR	FO	GP	GO	DC	IM	CR	FO	GP	GO	DC	IM	CR	FO
473105	0	0	0	0	0	50 (150)	0	0	0	20 (50)	0	50 (70,000)	3	1	0	50 (2,000)	0	50 (2,000,000)
459118	0	0	0	0	0	0	0	0	0	0	0	0	0	0	0	0	0	0
459144	0	0	0	0	0	50 (2000)	0	0	0	0	0	50 (20,000)	0	0	8	5	1	50 (250,000)
493334	0	0	0	13	0	50 (1000)	0	0	0	50 (125)	0	50 (20,000)	4	0	3	50 (3500)	0	50 (250,000)

	GP	GO	DC	IM	CR
459144			5	11	1
473105	3	1		61	
493334	4		3 analysed grains, NOT clinopyroxene	97	

Table 3. *Upper part: Number of identified indicator minerals obtained after processing at Overburden Drilling Management Ltd., Ontario, Canada. Numbers in brackets are estimated total number of grains in the picked sample. GP: garnet purple, GO: garnet orange, DC: chrome diopside (clinopyroxene), IM: ilmenite, CR: chromite, FO: olivine. Lower part: Number of grains analysed for major elements using the JEOL electron microprobe at Institute of Geography and Geology, Copenhagen University (Karina K. Sand, unpublished data).*

The chemical data showed that many of the analysed grains are mantle derived, and a few of them may have been derived from depths, where diamonds are stable.

Age determination

Before the project investigations were initiated, a preliminary age of 158 ± 2 Ma was available for a zircon within a loose block of a carbonatite breccia. The age determinations carried out as part of the project (Sebastian Tappe, unpublished data) confirm the Late Jurassic age of the complex and suggest that the UML dykes are slightly older than the main carbonatite phases:

Carbonatite (sövite) '488511' 152.1 ± 2.3 Ma (2-sigma); U-Pb zircon
 UML (aillikite) '488520' 159.5 ± 5.9 Ma (2-sigma); U-Pb perovskite
 UML (aillikite) '488546' 162.4 ± 1.4 Ma (2-sigma); U-Pb perovskite
 UML (aillikite) '488548' 165.2 ± 4.3 Ma (2-sigma); U-Pb perovskite

Mineralisation

Apatite appears to have an irregular distribution and apatite rich bands have been observed and sampled (Figure 22). The highest concentration of phosphorus measured in a rock sample is 10.84 % P_2O_5 (Table 4) and highest content of a scree sample is 14.4 % P_2O_5 (Table 4). Also several stream sediment samples collected in the creeks have contents above 3 % P_2O_5 indicating that apatite enrichment is not uncommon (Figure 21).

Surface accumulations of carbonatite pebbles with iron or manganese oxide/hydroxide coatings were seen at several sites (Figure 23 and 24), and were found to be radioactive. Besides uranium and/or thorium, these occurrences have high concentrations of barium, strontium, zinc and rare earth elements (see Ce values in Figure 21 and maximum values in Table 4). The origin of the mineralised pebbles is not known. However, one similar type of mineralisation is seen in one of the exposed creek sections and appears as a late narrow rusty vein with elevated radioactivity. Late hydrothermal veining is a likely way to form such kind of mineralisation. The gamma-spectrometer measurements show that anomalously high concentrations of thorium occur near the western contact with the country rocks. The radioactive pebble fields with rusty brown to black-coated pebbles could have been derived from occurrences near that contact and have been brought to their present position by downhill soil movement.

Concentrations of niobium reach maximum of 2044 ppm in a sample of dolomitic carbonatite, and several stream samples have between 500 and 750 ppm niobium (Figure 22). The mineral host for the niobium has not been identified, although pyrochlore has been looked for in thin sections of carbonatite samples. Tantalum is recorded in interesting concentrations up to 163 ppm in a sample of dolomitic carbonatite. This sample does not have high niobium, but has the highest recorded uranium concentration (169 ppm), so that it is suspected that Ta values are biased in samples with high uranium. Therefore, independent analyses (preferably by X-ray fluorescence spectrometry) are required to ascertain if such tantalum values are reliable. The samples with high niobium and tantalum were collected as samples of carbonatite – not as any recognised mineralisation.

Figure 25 shows the location of the strongest anomalies. These are sites where follow-up investigations are warranted to further determine the nature of the mineralisation.

Surface samples (55)						Mineralised rock samples (16)	
Element	Unit	Median	95th perc	Maximum	504961	Element	Maximum
Ag	ppm	1.0	1.4	1.4	<0.5	As	47
Al	%	5.2	7.4	7.9	5.03	Ba	73600
As	ppm	8	22	161	161	Be	43
Ba	ppm	1463	5248	7788	7788	Li	102
Be	ppm	9	23	52	6	Mn	13516
Bi	ppm	1.2	2.4	2.5	2.5	Mo	161
Ca	%	6.3	10.9	22.0	4.68	Nb	2044
Cd	ppm	0.6	1.1	1.3	1.3	P	28023
Ce	ppm	494	1623	3129	2238	P ₂ O ₅	6.42
Co	ppm	22	48	80	16	Pb	308
Cr	ppm	79	161	390	67.9	Sb	10.6
Cu	ppm	29	60	103	63.4	Sn	7.0
Fe	%	5.6	8.6	12.4	10.8	Sr	14353
Hf	ppm	4	7	20	3.2	Ta	163
K	%	2.1	3.9	4.5	1.49	Th	1160
La	ppm	239	825	1669	1013	U	169
Li	ppm	27	62	98	17.4	Y	761
Mg	%	3.0	6.4	10.8	1.62	Zn	2245
Mn	ppm	1896	4283	11151	11151	Zr	404
Mo	ppm	6	27	133	133.3	La	3190
Na	%	1.6	2.6	3.1	1.7	Ce	13300
Nb	ppm	305	565	750	425.8	Nd	5760
Ni	ppm	47	82	160	46.9	Sm	583
P	%	0.8	2.1	6.3	0.36	Eu	121
P ₂ O ₅	%	1.8	4.8	14.4	0.82	Tb	44
Pb	ppm	36	102	242	241.8	Yb	12.0
Rb	ppm	69	108	147	51.2	Lu	1.7
Sb	ppm	0.8	2	3	1.7		
Sc	ppm	23	36	74	19		
Sn	ppm	2.3	6	7	1.9		
Sr	ppm	1613	3697	6190	4530		
Ta	ppm	14	36	53	6.6		
Th	ppm	59	323	1118	1117.8		
Ti	%	0.2	0.3	0.5	0.165		
U	ppm	8.4	36	243	4.1		
V	ppm	74	106	186	37		
W	ppm	1.4	3.4	5.1	1.4		
Y	ppm	71	130	137	108.1		
Zn	ppm	172	375	976	976		
Zr	ppm	153	282	746	129.2		

Table 4. Summary statistical parameters for surface samples, values obtained in the most anomalous sample (soil sample 504961), and maximum values obtained in rock samples. Number of samples in parentheses.

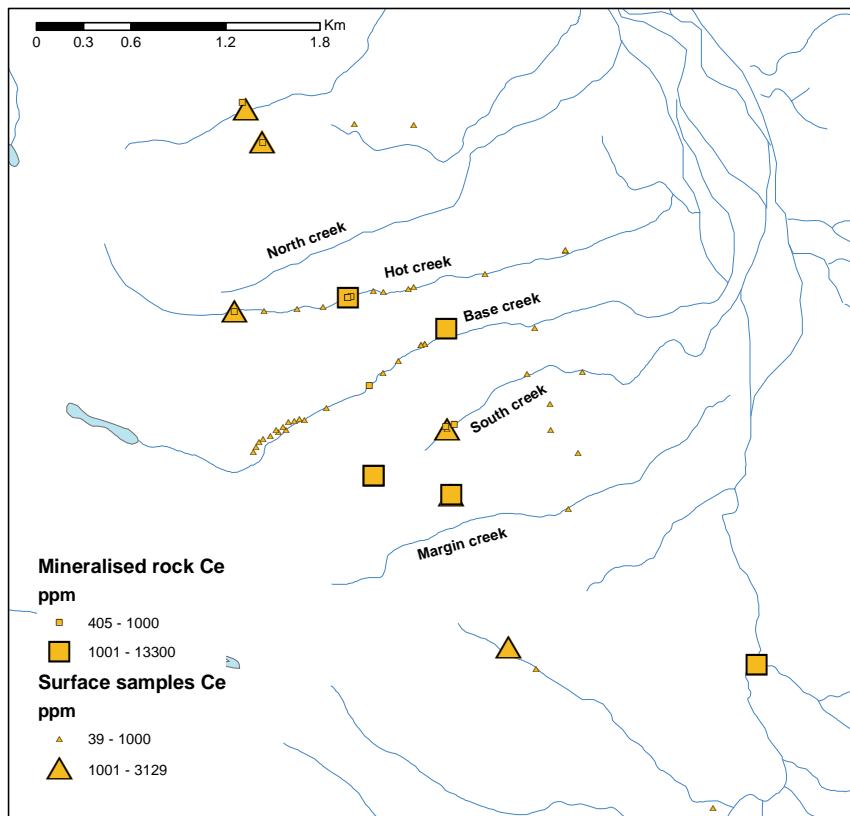
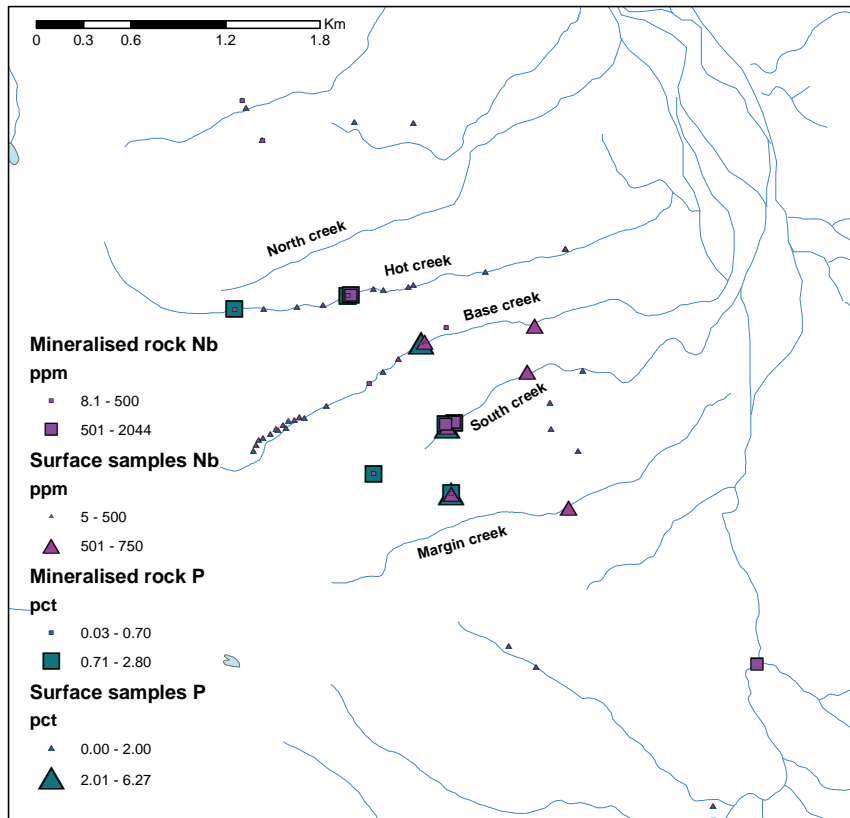


Figure 21. Distribution of high concentrations of niobium, phosphorus and cerium in surface, i.e. stream sediment, soil and sree. and in mineralised rock samples.



Figure 22. *Abundant greenish-grey apatite crystals in brownish dolomitic carbonatite.*



Figure 23. *Field of rusty carbonatite pebbles with elevated radioactivity on surface of slope.*



Figure 24. Close-up of coated carbonatite pebbles from radioactive pebblefield; iron oxide at left, manganese oxide at right.

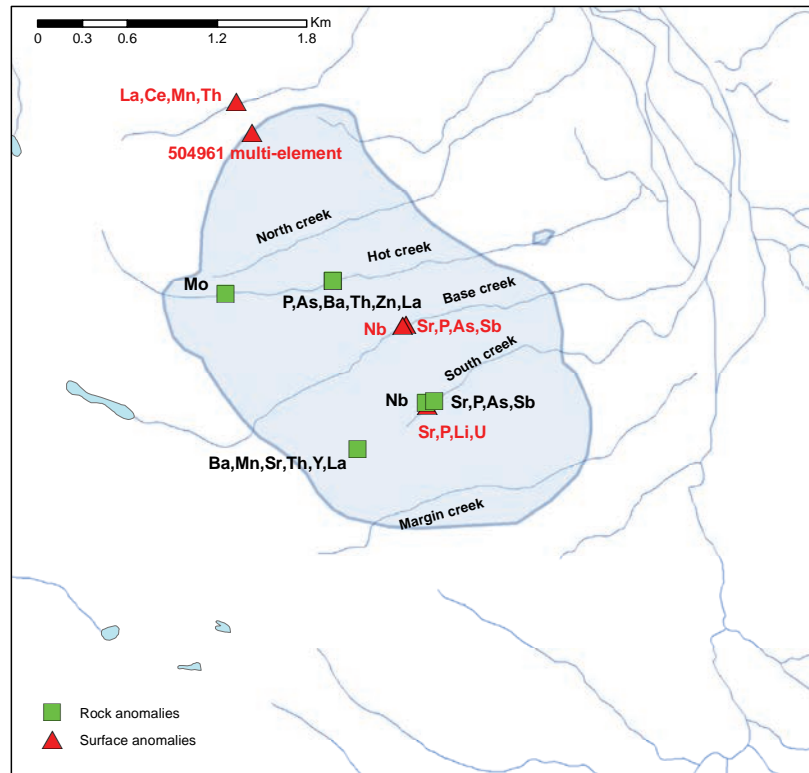


Figure 25. Outline of carbonatite core areas with location of strongest anomalies in rock and surface samples.

Economic potential

Carbonatite

Like other carbonatite complexes, Tikiusaaq is enriched in calcium, magnesium, barium, phosphorus, niobium, tantalum, yttrium and rare earth elements. Carbonatites are generally exploration targets for one or more of these commodities, and in a few cases exploitation has occurred (Siilinjärvi, Finland, and Palabora, South Africa) for apatite (phosphorus), copper, calcite, dolomite, mica.

Looking at the chemistry of the samples collected from Tikiusaaq, apatite (phosphorus) and perhaps REE could be of economic interest. In view of the increasing demand for nuclear fuel, even U and Th may be of interest. However, also surprisingly high concentrations of lithium (98 ppm in a sample of scree from radioactive fenite, and 101 ppm in radioactive gravel) and beryllium (33 ppm in each of two samples of brecciating carbonatite) were obtained. Thus in this project clear signs have been obtained of late veining and hydrothermal activity that have led to mineralisation. More prospecting and subsurface methods are warranted to further assess the size and grade of mineralised sites.

Ultramafic lamprophyre

The identification of (few) high-pressure minerals in samples of UML is encouraging and indicate a moderate diamond potential, although the lack of visible xenoliths in examined blocks and dykes of UML is less favourable. The most important information regarding the diamond potential is that the presence of Tikiusaaq proves that tectonic disturbances during the Late Jurassic have allowed melts of mantle origin access to the surface or near surface. This opens a possibility that diamond-bearing kimberlites have penetrated the crust elsewhere in the West Greenland.

Conclusion and recommendation

The size, exposure, main structure and composition of the Jurassic Tikiusaaq complex and ultramafic dykes have been established during a combination of field observations, gamma-spectrometry, mineralogical and chemical analyses of rock and surface material, and use of remote sensing data. The spatial distribution of acquired parameters and data has been studied and presented using GIS (Geographical Information System) software.

It is concluded that the Tikiusaaq carbonatite is equal in size, composition and mineralisation to the coeval and better studied and explored Qaqarssuk carbonatite east of Maniitsoq, and the discovery has enlarged the area affected by initial continental break-up along the Labrador Sea considerably.

An initial assessment of the economic potential has been based on observed and analysed mineralisation and geochemical anomalies. Enrichments in apatite and elements including barium, strontium, rare earth elements, thorium, uranium, niobium, tantalum, lithium, beryllium and manganese were recorded. However, intensive prospecting and excavation will be needed to find and substantiate the size and grade of any mineral occurrence within and in the margins of the carbonatite.

A moderate to low diamond potential has been estimated based on a few samples of ultramafic lamprophyre dykes. However, the area west of the carbonatite has not been searched for occurrences of ultramafic dykes within this project, and considering that dyke emplacement usually affects large areas, it is possible that more dykes and even some containing more mantle material occur further away from the carbonatite complex.

References

- Knudsen, C. 1991: Petrology, geochemistry and economic geology of the Qaqarssuk carbonatite complex, southern West Greenland. Monograph Series of Mineral Deposits **29**, 110.
- Larsen, L.M. & Rex, D.C. 1992: A review of the 2500 Ma span of alkaline-ultramafic, potassic and carbonatitic magmatism in West Greenland. Lithos **28**, 367–402.
- Secher, K. & Larsen, L.M. 1980: Geology and mineralogy of the Sarfartôq carbonatite complex, southern West Greenland. Lithos **13**, 199–212.
- Stendal, H., Nielsen, B.M., Secher, K. & Steenfelt, A. 2004: Mineral resources of the Precambrian shield of central West Greenland (66° to 70°15'N). Part 2. Mineral occurrences. Danmarks og Grønlands Geologiske Undersøgelse Rapport **2004/20**, 212 pp.

Appendix

Lithological and radiometric variation along profiles across carbonatite core area. Two parallel profiles were measured along the entire Base creek and along the upper part of South creek, one along the bottom of the scree and the other on top of the overburden (termed low and high, respectively, in the headings on the diagrams).

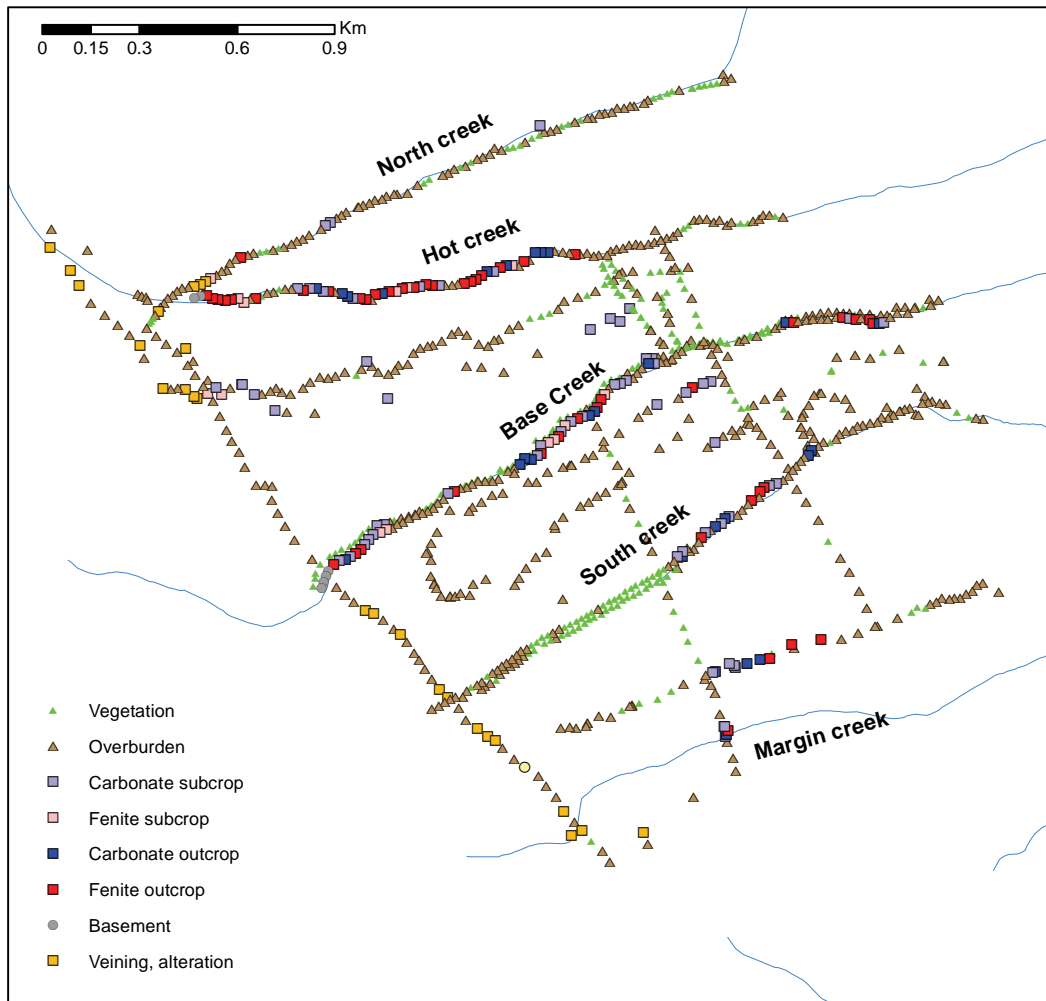
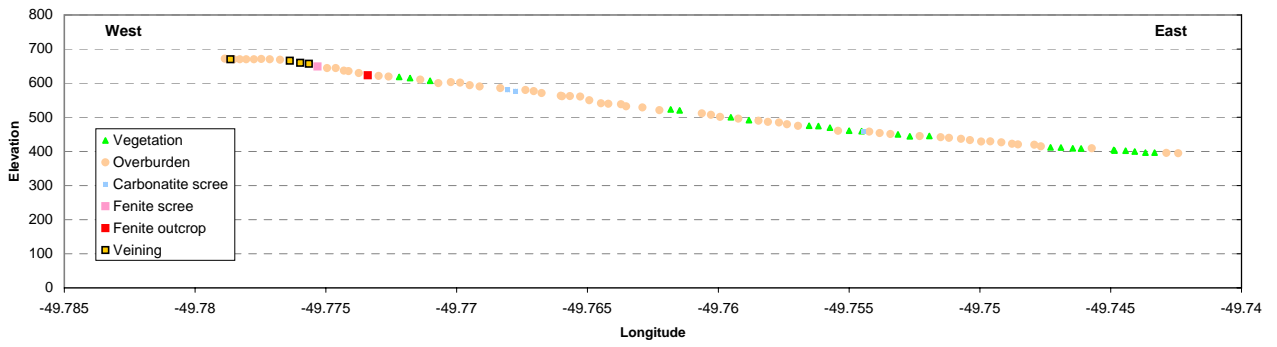
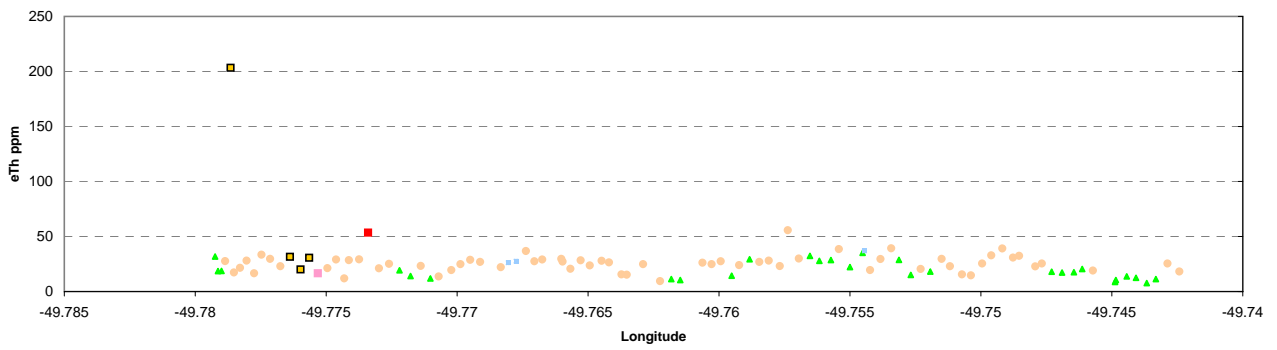


Figure A1. Profile location and names.

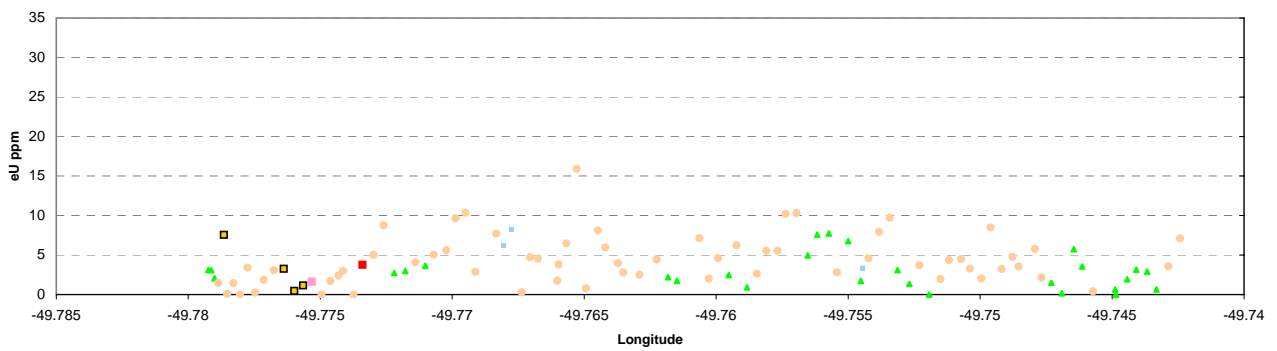
North creek profile



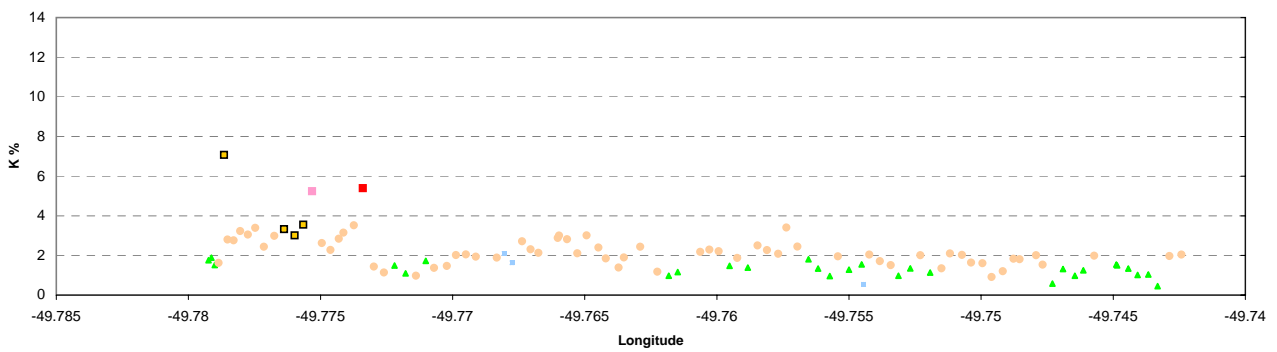
North creek Thorium



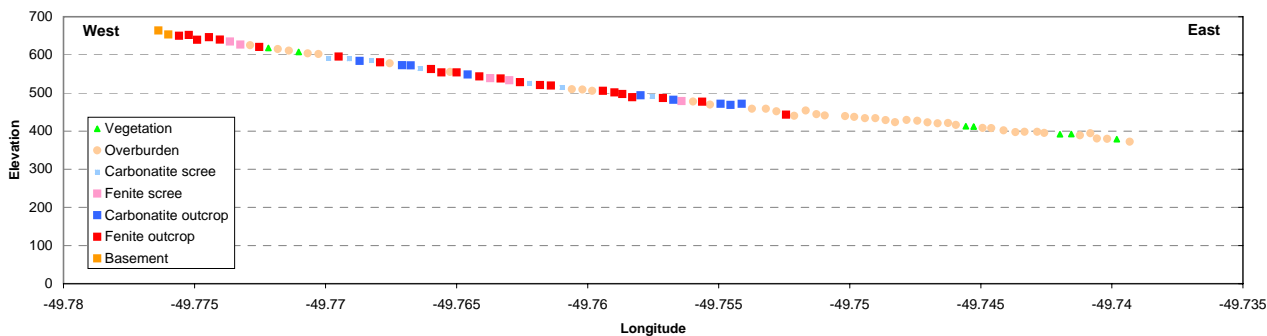
North creek Uranium



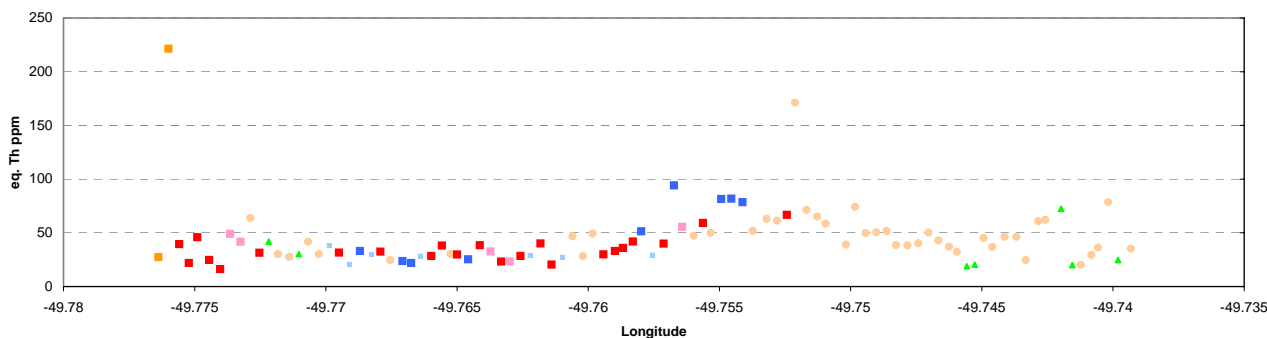
North creek Potassium



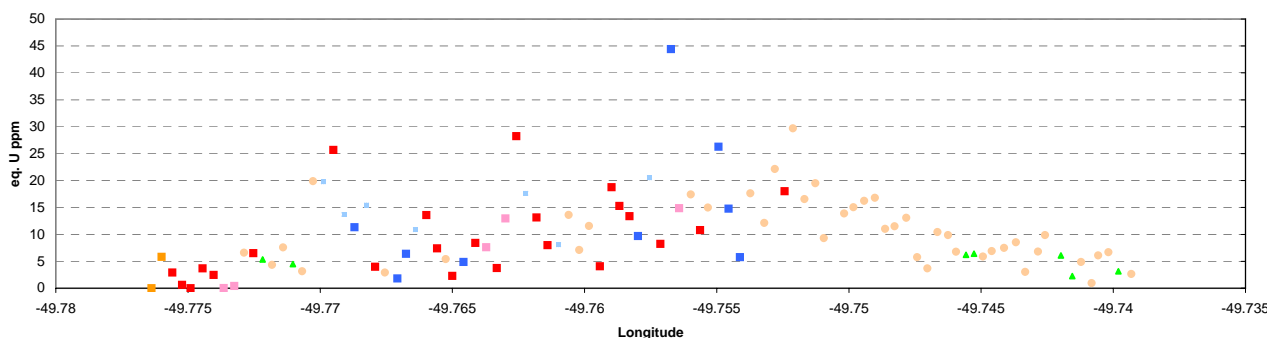
Hot creek profile



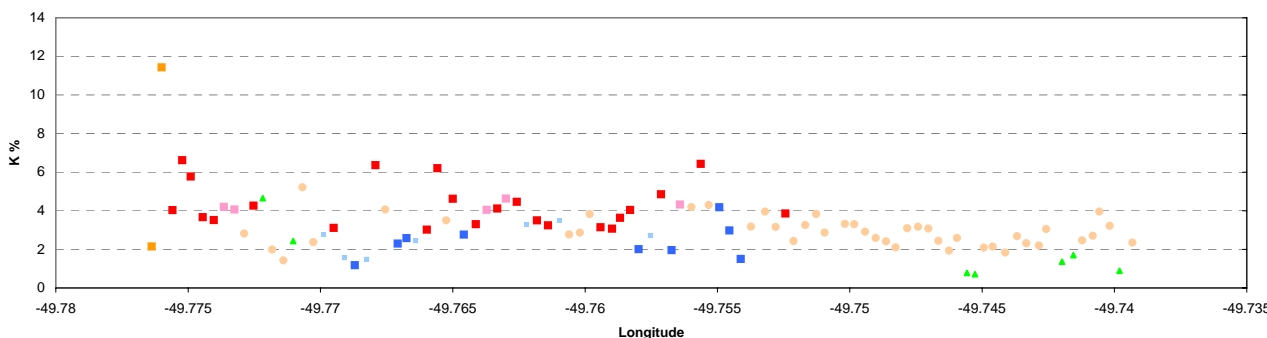
Hot creek Thorium



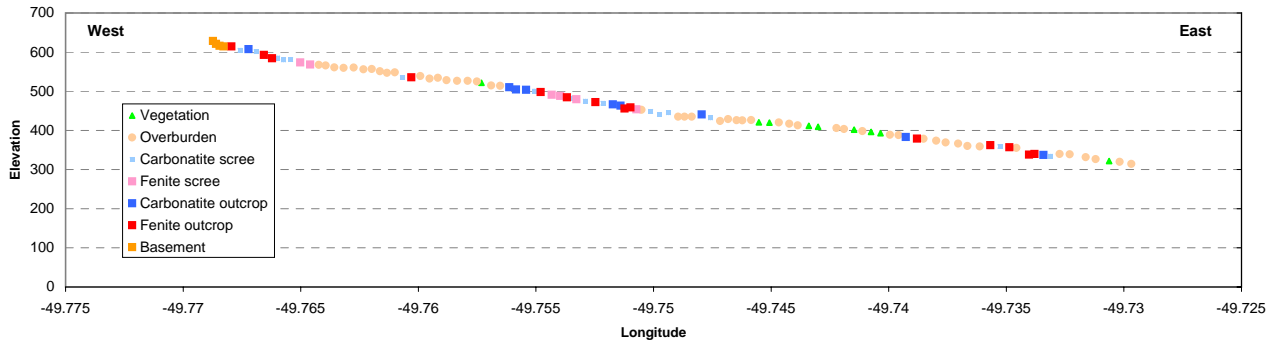
Hot creek Uranium



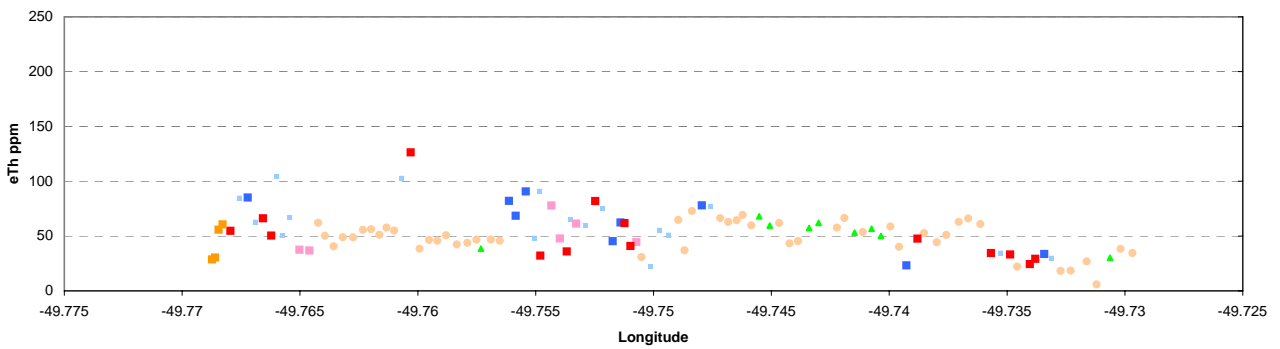
Hot creek Potassium



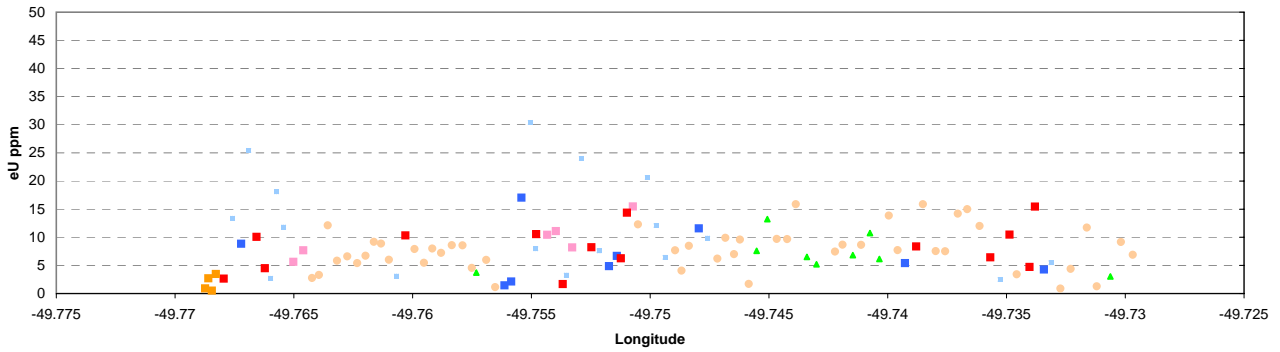
Base creek low profile



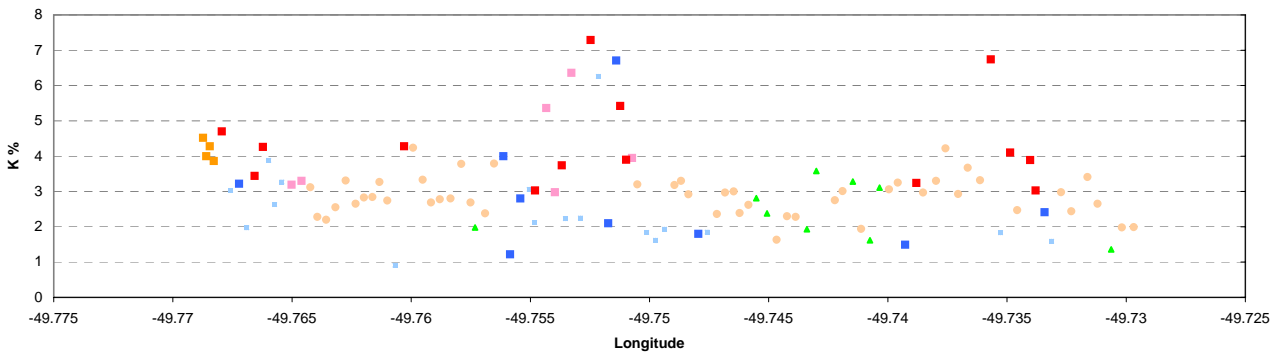
Base creek low Thorium



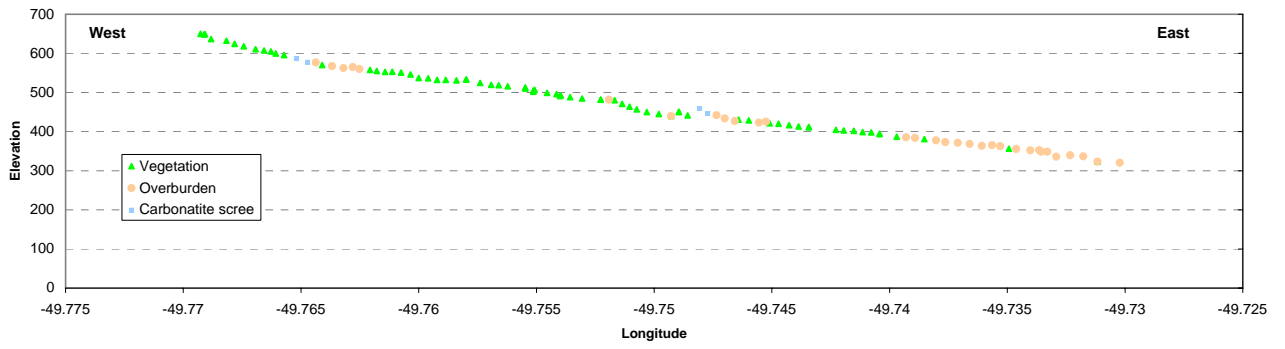
Base creek low Uranium



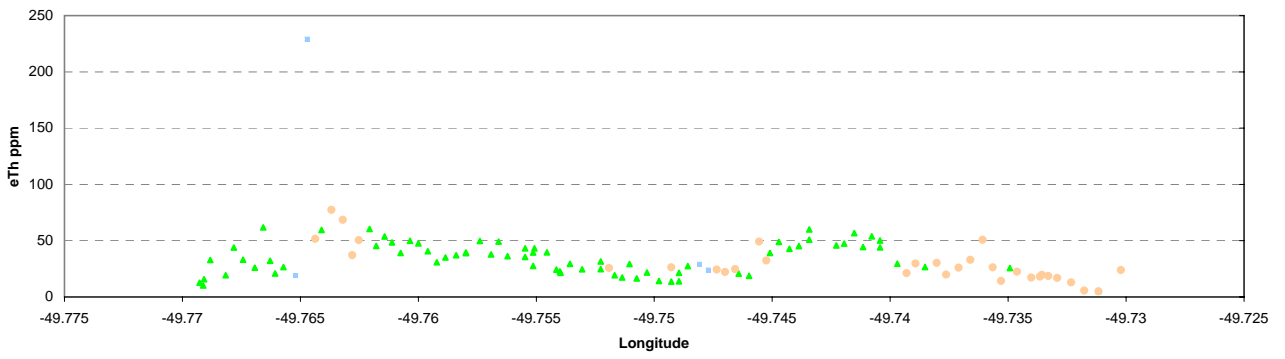
Base creek low Potassium



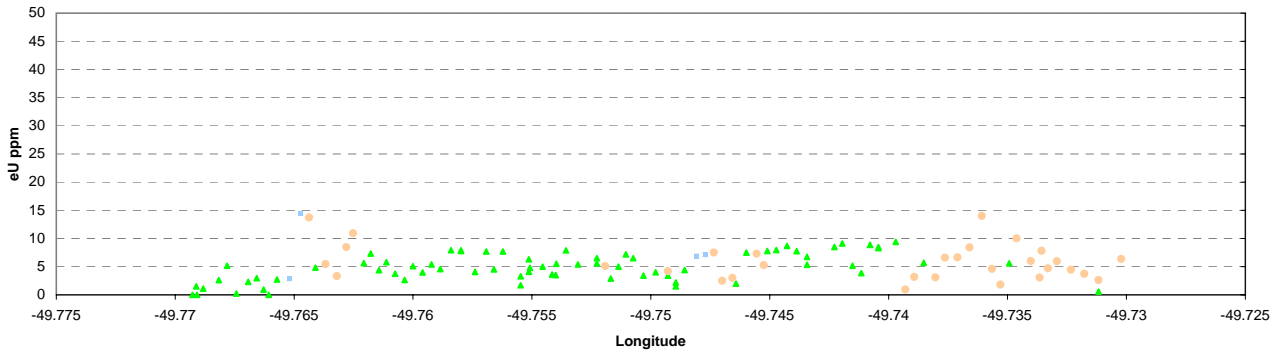
Base creek high profile



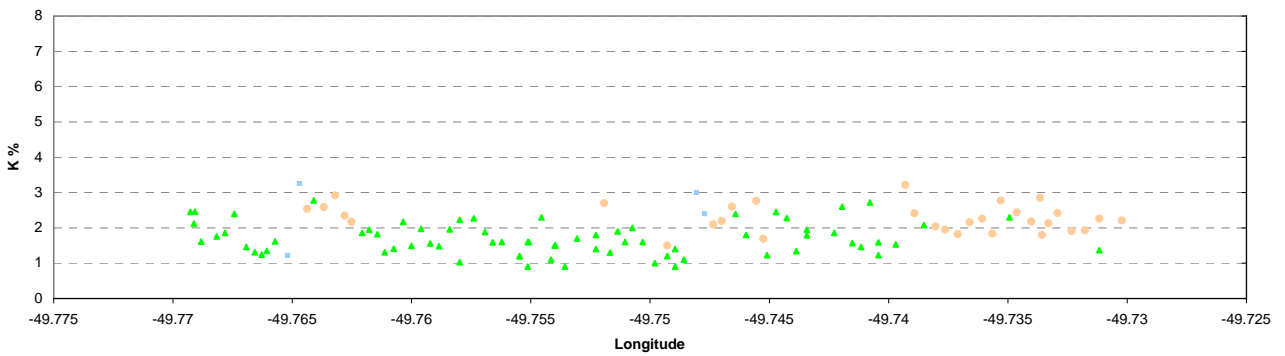
Base creek high Thorium



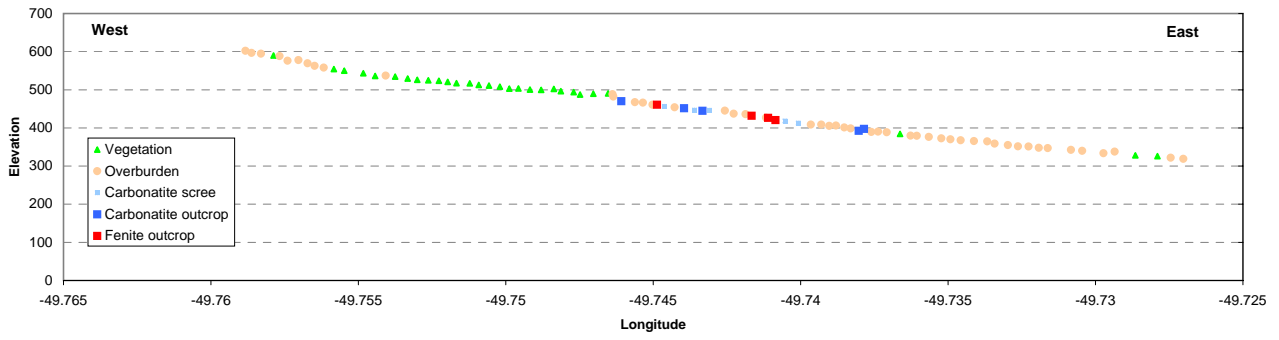
Base creek high Uranium



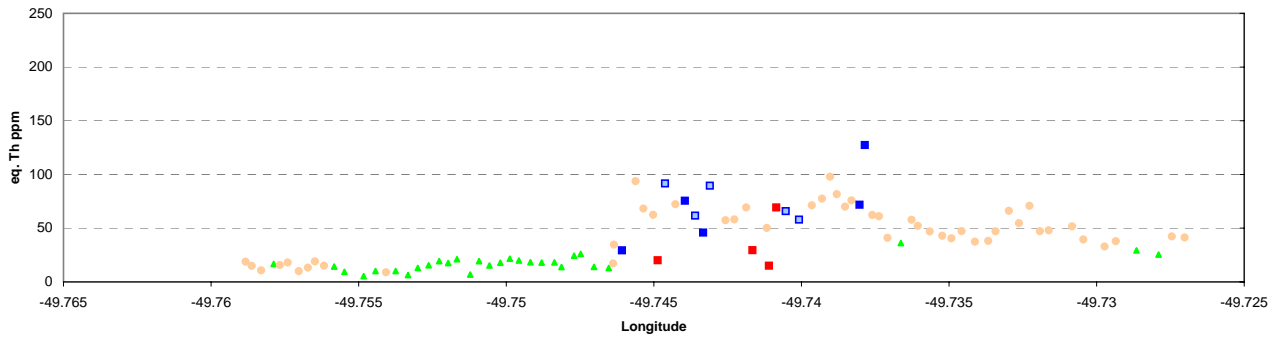
Base creek high Potassium



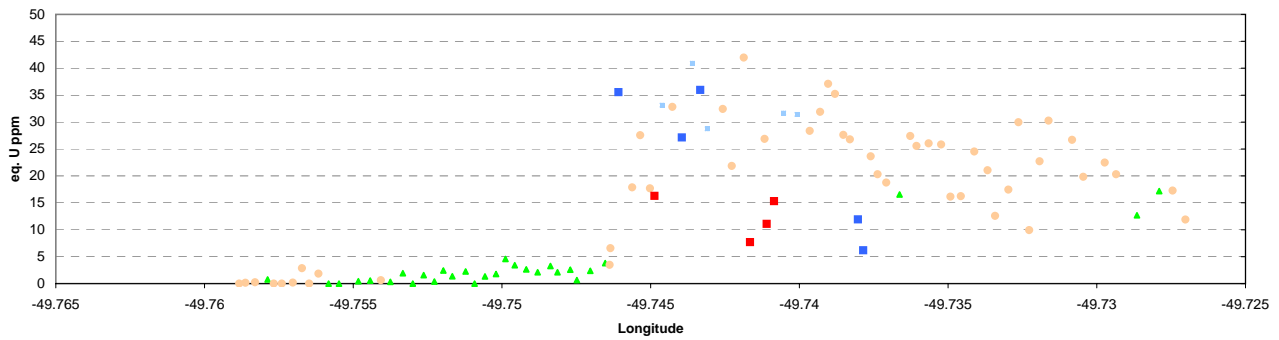
South creek low profile



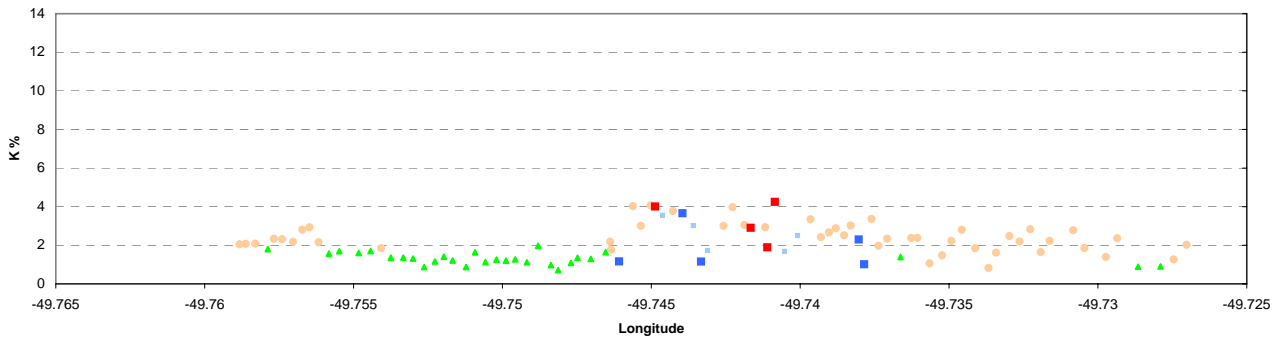
South creek low Thorium



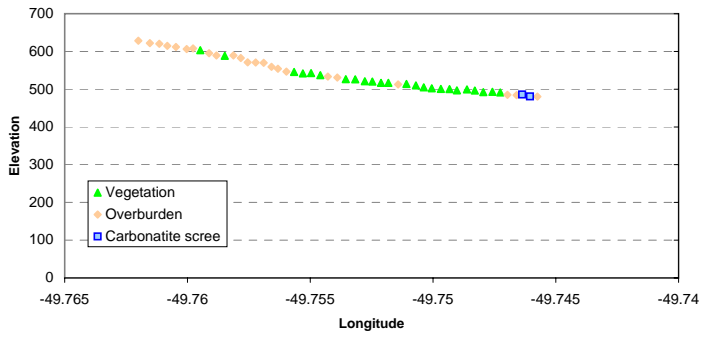
South creek low Uranium



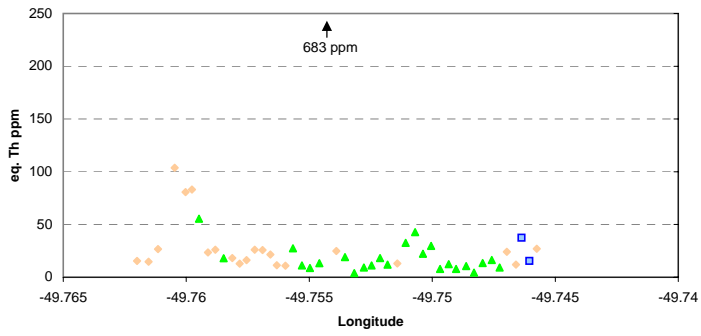
South creek low Potassium



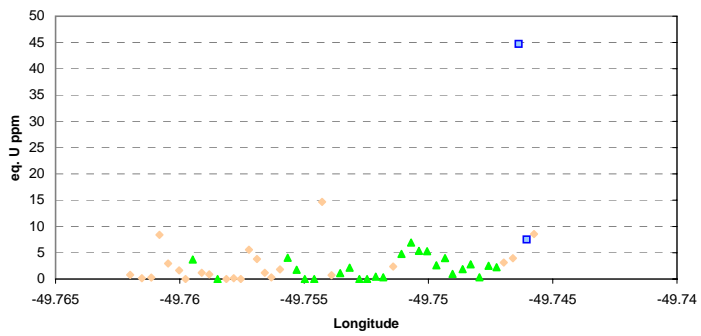
South creek high profile



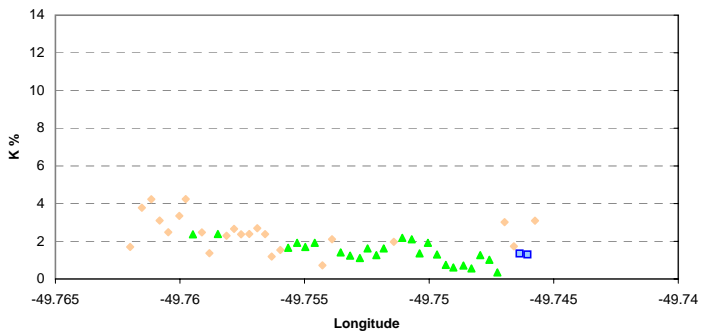
South creek high Thorium



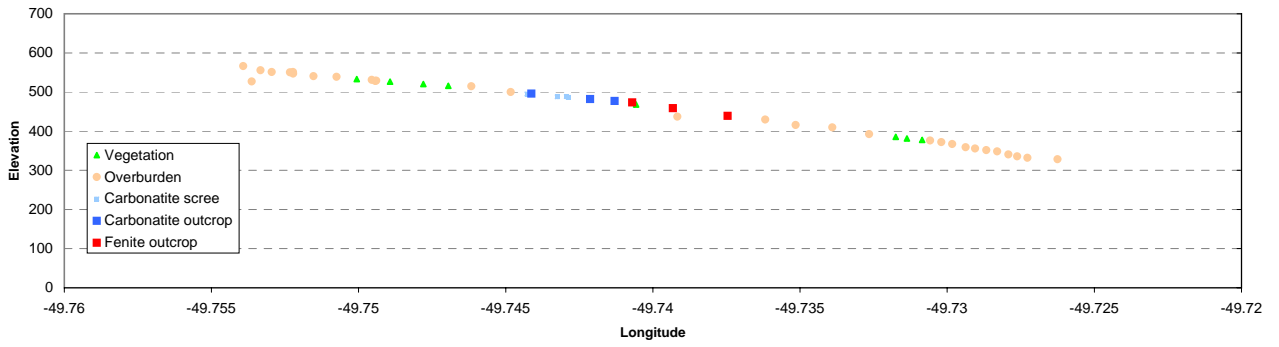
South creek high Uranium



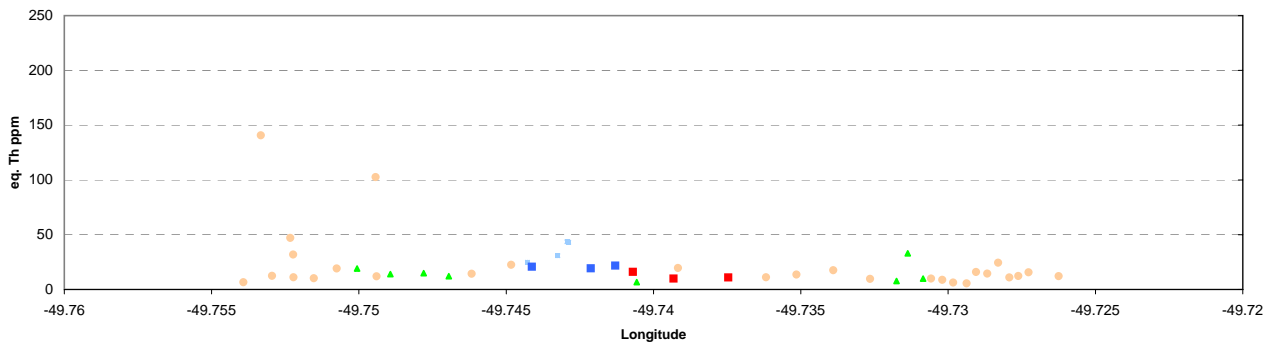
South creek high Potassium



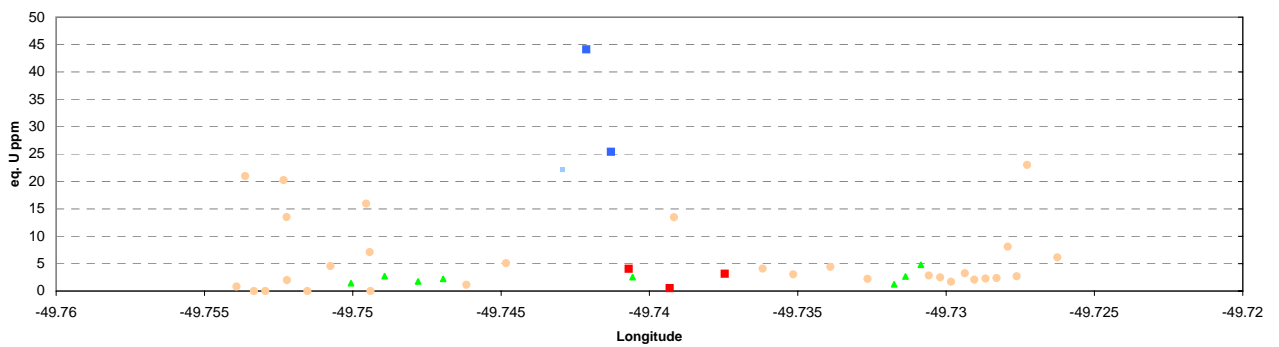
Margin creek profile



Margin creek Thorium



Margin creek Uranium



Margin creek Potassium

